Available online at www.CivileJournal.org

Civil Engineering Journal

(E-ISSN: 2476-3055; ISSN: 2676-6957)

Vol. 12, No. 06, June, 2026

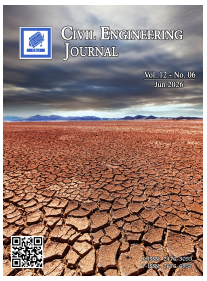

Stability of Pyramid-Shaped Gabion Armor Layers for Breakwaters

Muhammad [1*], Muhammad S. Pallu [1], Muhammad A. Thaha [1*], Hasdinar Umar [2]

[1] *Department of Civil Engineering, Hasanuddin University, South Sulawesi 91711, Indonesia.*

[2] *Department of Ocean Engineering, Hasanuddin University, South Sulawesi 91711, Indonesia.*

Received 19 January 2026; Revised 15 May 2026; Accepted 18 May 2026; Published 01 June 2026

Abstract

Breakwaters with pyramid-shaped gabion armor units represent an alternative coastal structure design that is permeable, economical, and environmentally friendly. This study aims to analyze the stability of pyramid-shaped gabion armor by examining damage levels, identifying key influential variables, and formulating inter-variable relationships to determine the stability coefficient (K_D) across various water level elevations. The research methodology employed physical modeling in a wave flume with variations in hydrodynamic parameters, including wave height (H_i), wave period (T), water depth (d), structural slope (θ), and the number of armor layers. The damage percentage was measured across various combinations of these parameters. The results indicate that wave steepness (H_i/L) significantly influences the structural damage rate during testing. Relative water depth (d/h) was found to significantly affect armor stability performance, particularly under emerged conditions (d/h < 1.0). The maximum damage level reached 6% under submerged conditions (d/h > 1.0) due to increased drag and lift forces. At the established damage criterion (1% damage), the stability coefficient (K_D) values ranged from 4.9 to 23.73, depending on the structural slope and the number of pyramid gabion armor layers. Pyramid-shaped gabion units demonstrate stability performance comparable to that of conventional artificial armor units, such as Tetrapods or Dolos, offering a highly efficient and cost-effective solution for sustainable coastal engineering.

Keywords: Pyramid Gabion Armor; Armor Layer Stability; Wave Deformation; Relative Depth.

1. Introduction

Coastal erosion is a serious problem that causes shoreline changes and can cause widespread economic, social, and environmental losses. Delayed intervention may exacerbate structural damage, necessitating rapid and appropriate mitigation measures. Before determining the type of coastal protection structures, it is important to identify the main causes of erosion. Based on these causes, mitigation strategies can be designed through the construction of coastal protection structures, beach nourishment, or integrated beach management. Shore structure selection should align with protection goals, whether that is restoration or maintenance of the shoreline. Some common methods include the construction of revetments, groins, jetties, and breakwaters, which serve to strengthen the shoreline, reduce wave energy, regulate sediment transport, or increase sediment supply. Construction materials range from permeable to impermeable options. Boulders are a commonly used material, but their availability is increasingly limited due to the difficulty of obtaining blasting permits in mountainous areas. This condition encourages innovation in the utilization of alternative materials, such as medium and small stones, which can be used as fill for breakwaters.

To ensure effective coastal protection, the stability of the protective layer of the breakwater is very important. One of the key parameters is the stability coefficient *(K_D)*, which is affected by material properties (shape, roughness, degree of interlocking), wave conditions, and structural configuration. According to Rohani et al. [1], the value of K_D increases with increasing stability number, wave steepness, and relative depth, but decreases for structures with gentler slopes.

* Corresponding author: muhammad21d@student.unhas.ac.id; athaha@unhas.ac.id

https://doi.org/10.28991/CEJ-2026-012-06-02

Gabion breakwaters are characterized by their permeability, which effectively attenuates wave energy through a complex dissipation mechanism. The structural stability of these units is primarily governed by the physical properties of the fill material and the geometric arrangement of the assembly [2, 3]. Additionally, hydrodynamic conditions and wave characteristics play a critical role in determining the long-term performance of the structure [4, 5]. Recent studies suggest that utilizing size-graded stones can significantly enhance interlocking capacity [6]. Furthermore, specific configurations, such as stepped or curved gabions, have demonstrated superior energy dissipation compared to standard designs [7]. Beyond their hydraulic performance, gabion structures offer substantial advantages in terms of cost-effectiveness, rapid construction, and environmental sustainability [8].

Although various artificial armor units, such as Tetrapods and Xblocs, have been extensively studied and widely applied in breakwater construction, the use of pyramid-shaped gabions remains relatively underexplored, particularly with respect to their hydrodynamic stability under different submergence levels. Classical formulations proposed by Hudson (1959) [9] and later refined by Van der Meer (1987) [10] indicated that armor layer stability is primarily governed by unit weight, wave characteristics, and the interlocking capacity between individual elements.

However, most previous studies have focused on rigid, massive concrete armor units, while permeable systems such as gabions (characterized by higher porosity and structural flexibility) have not been systematically evaluated within the framework of the stability coefficient (K_D). Theoretically, a pyramid geometry may increase the contact surface area between units, lower the overall center of gravity of the system, and enhance mechanical interlocking compared to conventional cubic gabions. Nevertheless, experimental evidence assessing the performance of this geometry under varying water level conditions (emerged, low crest (LC), and submerged) remains limited.

By addressing this research gap, the present study proposes a breakwater model composed of pyramid-shaped gabion units filled with medium-sized stones that are larger than the gabion mesh openings. The objective is to evaluate structural stability under wave loading by identifying the key governing variables and formulating empirical relationships among them to determine the stability coefficient (K_D), thereby providing practical guidance for coastal engineering design.

2. Theoretical Basis

2.1. Coastal Hydraulics

Waves are classified into three regimes—shallow, transitional, and deep water—based on the ratio of water depth to wavelength *(d/L)* [11]. The specific boundaries defining these classifications are summarized in Table 1.

Table 1. Classification of ocean waves based on relative depth

Classification	*d/L*	$2\pi d/L$	$tanh = (2\pi d/L)$
Deep water	> 1/2	> π	≈ 1
Transitional water	1/20 to 1/2	1/4 - π	$tanh(2\pi d/L)$
Shallow water	< 1/20	< 1/4	$\approx (2\pi d/L)$

This study employs Airy wave theory (linear wave theory) to analyze wave characteristics. The free surface profile (η) is expressed as a function of spatial position (x) and time (t) in the following form:

$$\eta\,(x,t) = \frac{H}{2}\cos(kx - \sigma t) \tag{1}$$

Equation 1 demonstrates that water level fluctuations are periodic and sinusoidal, representing a progressive wave traveling in the positive x-direction. The wave propagation speed (C) and the wavelength (L) are determined using Equations 2 and 3, respectively [12]:

$$C = \frac{gT}{2\pi}\tanh\frac{2\pi d}{L} = \frac{gT}{2\pi}\tanh kd \tag{2}$$

$$L = \frac{gT^2}{2\pi}\tanh\frac{2\pi d}{L} = \frac{gT^2}{2\pi}\ tanh\, kd \tag{3}$$

In these equations, H denotes the incident wave height (m), while k represents the wave number ($2\pi/L$) (rad/m) and σ signifies the angular wave frequency ($2\pi/T$) (rad/s). Additionally, d refers to the water depth (m), T is the wave period (s), and x and t correspond to the spatial and temporal coordinates, respectively.

2.2. Stability of Primary Armor

The fundamental equation for determining the stability of rubble-mound breakwater armor was developed by Hudson [9]. Based on the criteria of zero damage and no overtopping, the relationship between wave force and the required weight of the armor unit is formulated as follows:

$$W = \frac{\gamma_r H^3}{K_D\left(\frac{\gamma_r}{\gamma_a}-1\right)^3 Cot\theta} \quad (4)$$

In this expression, W denotes the weight of the armor unit (ton), γ_r is the specific weight of the armor material (t/m^3), H represents the design wave height (m), θ is the slope angle of the breakwater, and K_D is the dimensionless stability coefficient. Correspondingly, the stability coefficient can be derived as:

$$K_D = \frac{\gamma_r H^3}{W\left(\frac{\gamma_r}{\gamma_a}-1\right)^3 Cot\theta} \quad (5)$$

Values for K_D across various armor types are documented in the Shore Protection Manual [11, 13], where a higher K_D value signifies superior structural resistance to wave action. According to Hudson's formulation, stability is governed by four key parameters: wave characteristics, material density, fluid properties, and structural geometry. While Thaha et al. [14] suggest that stability can be achieved using smaller stones by employing an S-shaped geometric slope with an extended toe, this configuration often requires a significantly higher volume of material.

The choice of armor unit is the primary determinant of the stability coefficient (K_D), which directly dictates the nominal weight required to withstand incident wave energy. Comparative analysis of various manufactured units reveals distinct performance characteristics: Tetrapods and quadripods demonstrate reliable stability with K_D values between 7.8 and 8.0 for non-breaking wave conditions. Tribars exhibit variable stability depending on placement; random placement in two layers yields K_D values of 9.0–10.0, whereas uniform single-layer placement significantly enhances efficiency, reaching K_D values of 12.0–15.0. Dolos units provide the highest stability due to their exceptional interlocking capacity, with K_D values reaching up to 31.8 under non-breaking waves, although this stability may decrease by approximately 50% at the breakwater trunk. Finally, modified hexapods and cubes offer stability slightly exceeding that of Tetrapods (K_D 8.0–9.5), while modified cubes (K_D 6.5–7.5) outperform natural quarry stone but remain less effective than multi-legged interlocking units.

2.3. Theoretical Framework of Pyramid Gabion Stability

The theoretical approach of this research is rooted in the balance of hydrodynamic forces acting on a permeable armor unit. Unlike solid concrete units, the stability of a pyramid-shaped gabion is governed not only by its self-weight but also by its high internal porosity and mechanical interlocking. According to the Hudson formula, stability is a function of the drag (F_D), lift (F_L), and inertia forces (F_I) exerted by waves.

In the case of a pyramid geometry, the tapered shape provides a lower center of gravity and increases the contact surface area between adjacent units, which enhances the friction force (F_f). Mathematically, the stability can be expressed through the equilibrium equation where the resisting forces (gravity and interlocking) must exceed the driving forces (buoyancy and hydrodynamic pressure). Furthermore, the permeability of the gabion allows for significant energy dissipation through internal flow turbulence, reducing the net pressure gradient across the armor layer. This study focuses on quantifying the stability coefficient (K_D) as a lumped parameter that represents these complex theoretical interactions under varying relative water depths (d/h).

2.4. Characteristics of Wave Deformation

Wave characteristics undergo significant transformations due to variations in water depth, particularly in shallow water regions. These parameters are primarily altered by shoaling, refraction, and wave breaking. To analyze the interaction between incident waves and coastal structures, three key parameters are calculated: transmission, reflection, and wave energy dissipation. The capacity of a structure to reflect wave energy is quantified by the reflection coefficient (K_r), defined as the ratio of the reflected wave height (H_r) to the incident wave height (H_i):

$$K_r = \frac{H_r}{H_i} = \sqrt{\frac{E_r}{E_i}} \quad (6)$$

where the reflection energy is $E_r = \frac{1}{8}\rho g H_r^2$ and the incident wave energy is $E_i = \frac{1}{8}\rho g H_i^2$. In these expressions, ρ represents the mass density of the fluid and g is the acceleration of gravity. The value of K_r ranges from 1.0 (total reflection) to 0 (no reflection). Reflection coefficients for various structures, typically estimated through experimental modeling, are summarized in Table 2 [11].

Table 2. Reflection coefficients for various coastal structures

Energy-Absorbing Structure Type	K_r
Vertical wall (crest above water level)	0.7 – 1.0
Vertical wall (submerged)	0.5 – 0.7
Sloping rubble-mound structure	0.3 – 0.5
Concrete block armor	0.3 – 0.5
Perforated vertical structures (with energy absorbers)	0.05 – 0.2

Wave transmission is characterized by the transmission coefficient (K_t), which represents the ratio of the transmitted wave height (H_t) to the incident wave height (H_i):

$$K_t = \frac{H_t}{H_i} = \sqrt{\frac{E_t}{E_i}} \quad (7)$$

Following the methodology of Horikawa (1978) [15], the amount of dissipated wave energy (K_d)—or the damping coefficient—is determined by subtracting the transmitted and reflected energy from the total incident energy:

$$K_d = \sqrt{1 - {K_t}^2 - {K_r}^2} \quad (8)$$

Under the influence of bottom friction, wave height decreases exponentially. Friction also reduces the wavelength and propagation speed. Consequently, an increase in the Darcy-Weisbach friction coefficient (f) results in enhanced wave height attenuation.

2.5. Physical Modeling

Laboratory experiments were conducted using physical gabion models to evaluate structural performance under diverse wave conditions. To ensure that the experimental data provides a valid representation of the prototype, the physical model must adhere to principles of similarity, specifically geometric, kinematic, and dynamic congruence [16]. Geometric similarity requires the model and prototype to be identical in shape, maintaining a constant ratio for all linear dimensions. This scale ratio is expressed as:

$$n_L = \frac{L_p}{L_m} \quad (9)$$

$$n_h = \frac{h_p}{h_m} \quad (10)$$

where, n_L is the length scale, n_h is the height scale, L_p is the length of the prototype, L_m is the length of the model, h_p is the height of the prototype, and h_m is the height of the model.

Kinematic similarity is achieved when geometric similarity is satisfied and the ratios of velocity and acceleration at corresponding points are equal. The scales for velocity (n_v), acceleration (n_a), discharge (n_Q), and time (n_t) are defined as follows:

$$n_v = \frac{v_p}{v_m} = \frac{n_L}{n_T} \quad \text{for speed} \quad (11)$$

$$n_a = \frac{a_p}{a_m} = \frac{n_L}{{n_T}^2} \quad \text{for acceleration} \quad (12)$$

$$n_Q = \frac{Q_p}{Q_m} = \frac{{n_L}^2}{n_T} \quad \text{for flow rate} \quad (13)$$

$$n_T = \frac{T_p}{T_m} \quad \text{for time} \quad (14)$$

Dynamic similarity requires that the ratio of all forces acting on the model and prototype (such as inertial, pressure, gravitational, and frictional forces) remains constant. For studies involving wave reflection and run-up, gravitational forces dominate. Therefore, this study employs Froude's Law using an undistorted model, where the length and height scales are identical. Under Froude scaling, the time scale (n_t) relates to the length scale as follows:

$$n_t = \sqrt{n_L} \quad (15)$$

2.6. Dimensional Analysis Method

Dimensionless numbers are used to express the relationship between parameters and are used to describe research results. Determining the dimensionless numbers can be done by dimensional analysis. The *Langhaar* method is the one used for this research because it is systematic and there are relatively few influential variables.

3. Research Methodology

3.1. Time and Location of Research

This research was conducted over a period of six months at the Hydraulics Laboratory in the Department of Civil Engineering at the Faculty of Engineering, Hasanuddin University in Gowa Regency.

3.2. Tools and Materials

Research was conducted on a multipurpose wave flume channel measuring 15 meters long and 0.3 meters wide. The effective depth of the channel is 46 cm. The generating machine consists of a main engine, a pulley used to adjust the rotation time of the disk connected to the stroke, which moves the wave generator flap. The wave flume and wave-generating unit are shown in Figure 1, and the data recording process unit is shown in Figure 2.

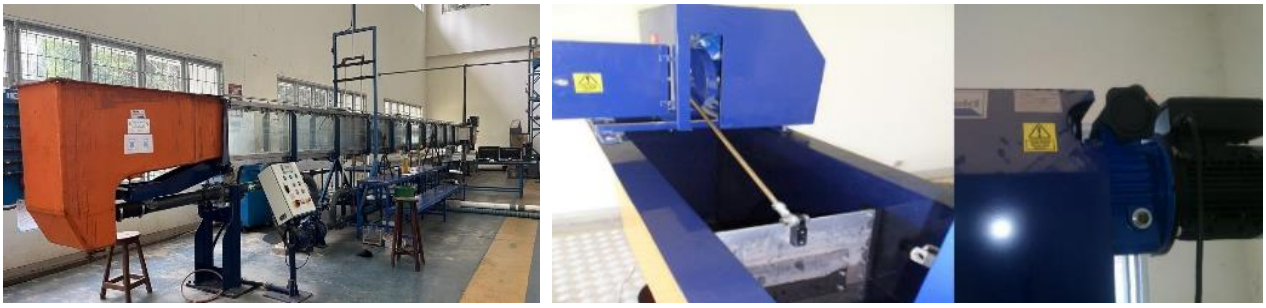

Figure 1. Wave flume and flap-type wave generating unit

Figure 2. Personal computer unit and oscilloscope software, Wave probe sensor set and buffer, Wave monitor with connecting cable, and Data acquisition

The Wave Probe Sensor Rod, which functions to capture mechanical signals in the form of water level fluctuations that move up and down. The principle works by capturing the signal to change the resistance value into a signal that is forwarded to the wave monitor. The Wave Monitor displays the dialogue signal received by the Wave Probe Sensor Rod. It is used to adjust the position of the signal so that it is located within the oscilloscope software. Data acquisition functions collect and convert mechanical signals into electrical signals to be read by the oscilloscope software. The materials used in making the pyramid shape gabion model are materials for assembling or making the physical model to be tested consisting of wire as a material for wrapping the gabion unit, crushed stone measuring 50 mm in diameter as gabion filling, thread and needle to tie the gabion unit, acrylic for making fine cores, glue and screws for assembling fine cores.

3.3. Damage Definition and Scale Effects

In this study, the threshold for structural stability is quantified through a precise definition of 'damage.' Following established experimental protocols for rubble-mound structures, damage is defined as the displacement of an individual gabion unit from its original position by a distance equal to or exceeding its characteristic nominal dimension (D_n). While minor rotations and vertical settlements were observed during the experiments, these were recorded as 'settlements' and were not categorized as damage unless they resulted in the exposure of the filter layer or the complete removal of the unit from the armor grid. This rigorous criteria ensures that the reported 1% damage threshold represents a conservative and reproducible measure of the structure's limit state.

Furthermore, while the physical model adheres to Froude's similarity law for gravity-dominated free-surface flow, the authors acknowledge the potential for viscous scale effects inherent in porous media such as gabions. To mitigate permeability distortions at a reduced scale, the stone filler size (d_{50}) was carefully selected to ensure that the flow within

the gabion cages remained within the turbulent regime. By maintaining a sufficiently high Reynolds number for the internal flow, the influence of scale effects on the stability coefficient (K_D) was minimized, ensuring that the laboratory observations provide a reliable proxy for prototype-scale performance.

3.4. Model Design

The determination of the geometry scale is adjusted to the capabilities and capacity of the wave flume in the laboratory, compared to the size of the prototype. In this study, undistorted models will be used. In the undistorted model, the geometry between the model and the prototype is the same. However, they are different sizes. This means there is a size or scale comparison. In this study, the planned water depth is assumed to be 2 m, 3 m, 4 m, 5 cm, 6 cm and 7 m, for the depth operated in the wave flume, namely 10 cm, 15 cm, 20 cm, 25 cm, 30 cm and 35 cm, so that the scale of the experiment is:

$$n_L = \frac{L_p}{L_m} = \frac{300}{15} = 20$$

The length scale (n_L) above applies to all distance scaling (length and height) in this study, including wave height *(H)*, thus:

$$n_L = n_H = 20$$

The length scale (n_L) is used in determining the dimensions of the model. For the determination of the wave period *(T)*, time scaling is used using Froude similarity using Equation 15.

$$n_t = \sqrt{n_L} = \sqrt{20} = 4.47$$

The complete model scale value can be seen in Table 3.

Table 3. Model scale used

Definition	Notation	Scale
Length scale	n_L	20
Height scale	n_H	20
Depth scale	n_d	20
Time scale	n_T	4.47

In physical wave modeling, scale effects inevitably arise due to the impossibility of maintaining all dimensionless force ratios—Froude, Reynolds, and Weber numbers—simultaneously between the model and the prototype. This study utilizes Froude Similarity at a geometric scale (n_L) of 1:20, as the primary phenomena involved, such as wave propagation, run-up, and armor stability, are gravity-dominated. To mitigate potential viscous scale effects inherent in permeable structures like gabions, the Reynolds number (*Re*) for the stone filler was maintained above the critical threshold ($Re_p > 10^3$) using the median stone diameter (d_{50}) as the characteristic length. This ensures that the hydraulic conductivity remains independent of viscous forces, thereby maintaining a turbulent flow regime within the gabion cages that accurately represents prototype conditions.

Furthermore, permeability distortion and surface tension effects were carefully addressed to ensure model validity. Following the approach suggested by Juul Jensen & Klinting (1983) [17], a scale correction was applied to the stone filler size to compensate for disproportionately high viscous forces at a small scale, ensuring proper energy dissipation within the porous pyramid-shaped units. To minimize Weber number influences on wave breaking and run-up, the minimum wave height was maintained above 2.0 cm. Additionally, the wire mesh was selected based on equivalent tensile strength and flexibility to simulate the "flexible-rigid" behavior of actual gabions, ensuring the model's structural confinement was not artificially stiffer than the prototype.

3.5. Model Shape and Dimensions

In this study, the physical model utilizes pyramid-shaped gabion armor units, each with a volume of 27.04 cm³. The experimental program encompasses several variations, including structure slope angles ($\tan\theta$) of 1:1.5 and 1:2, with a two-layer configuration applied to each slope. Specifically, for the 1:1.5 slope, the assembly consists of 164

units for a single layer and 350 units for two layers. For the 1:2 slope, the arrangement requires 180 units for a single layer and 380 units for two layers. The testing further considers five water depth variations (d) and three wave period variations (T). The core of the model is constructed from acrylic material, forming a trapezoidal structure with dimensions of 89.50 × 30 × 15 cm, specifically designed to accommodate the wave flume's geometry. The detailed cross-sectional view of the model is illustrated in the sketch in Figure 3, while the side, front, and top views are presented in Figure 4.

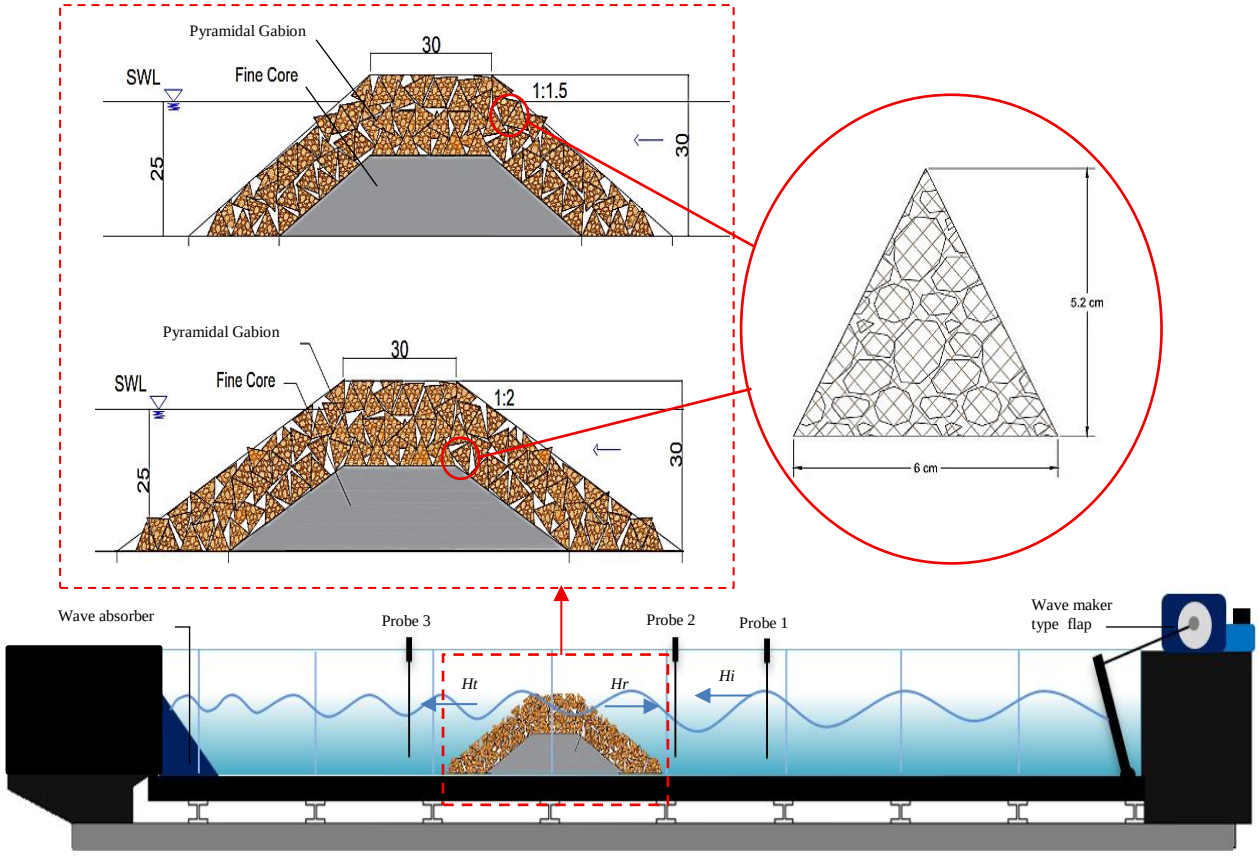

Figure 3. Sketch of the model in the wave flume with the placement position of the protected layer model of the pyramid-shaped gabion arrangement slope (θ = 1:1.5 and 1:2)

Figure 4. Side, front, and top views of the pyramid-shaped gabion protection layer model in the wave flume

The dimensions of the pyramid-shaped gabion structure models in this study consisted of 1-layer, 2-layer, and prototype models with varying structural parameters. The single-layer model has a thickness of 25 cm, while the double-layer model has a thickness of 30 cm, representing prototype dimensions of 5 m and 6 m thick. Both model variations have the same top width of 30 cm (6 m prototype), but the bottom width adjusts to the slope of the protective layer; at a slope of 1:1.5, the bottom width reaches 120 cm (24 m prototype), while at a slope of 1:2, the bottom width reaches 150 cm (30 m prototype).

3.6. Experimental Program and Variables

The experimental matrix was designed to evaluate the structural response of the pyramid gabion units under a wide range of hydraulic and structural conditions. The primary variables include the structure's slope ($cot\ \theta$), the number of armor layers, water depth (d), wave period (T), and wave stroke (S). The comprehensive set of simulation variables is summarized in Table 4.

Table 4. Matrix of experimental variables for hydraulic and structural parameters

Slope ($cot\,\theta$)	Armor Layer	Water Depth d (cm)	Wave Period T (s)	Wave Stroke S (cm)
1:1.5	One Layer	10, 15, 20, 25, 30	1.0, 1.1, 1.2	3; 5; 7; 9
1:1.5	Two Layer	15, 20, 25, 30, 35	1.0, 1.1, 1.2	3; 5; 7; 9
1:2	One Layer	10, 15, 20, 25, 30	1.0, 1.1, 1.2	3; 5; 7; 9
1:2	Two Layer	15, 20, 25, 30, 35	1.0, 1.1, 1.2	3; 5; 7; 9

As detailed in Table 4, the study investigated two distinct structural slopes, 1:1.5 and 1:2, to assess the influence of gradient on wave run-up and energy dissipation. For each slope, the armor units were arranged in both single-layer and double-layer configurations, allowing for a comparative analysis of interlocking performance and structural thickness.

The hydraulic conditions were systematically varied to simulate different coastal environments. Water depths (d) ranged from 10 cm to 35 cm, encompassing both emerged and submerged states relative to the structure's height. Wave characteristics were controlled by three wave periods (T)—1.0 s, 1.1 s, and 1.2 s—and four wave stroke levels (S) ranging from 3 cm to 9 cm. This combination of variables resulted in a robust dataset, enabling the derivation of the stability coefficient (K_D) under various wave steepness and submergence ratios.

3.7. Material Properties and Packing Characteristics

The armor layer consists of pyramid-shaped gabion units, each meticulously filled with crushed stone to ensure structural consistency. The stone filler possesses a bulk density (ρ_s) of 1,600 kg/m^3, providing the necessary mass to resist hydrodynamic forces. Each individual gabion unit has an average mass (W) of 0.03142 kg, which was maintained across all test samples to ensure a uniform distribution of weight within the armor layer. To characterize the internal structure of the gabions, the average porosity (n) was determined to be 0.445 (44.5%). This high level of porosity is critical for effective energy dissipation, as it allows for significant wave penetration and internal turbulence. The units were hand-packed to achieve this specific porosity and a consistent packing density, thereby minimizing variability in mechanical interlocking and ensuring that the calculated stability coefficients (K_D) accurately reflect the geometric performance of the pyramid design.

3.8. Research Flow Diagram

This experimental research was conducted in a laboratory using a wave flume, where a wave breaker model was placed in the middle of the channel and filled with water to the specified depth variations. The process began by setting the wave period using a variator and adjusting the positions of probes 1 and 2 at distances of ½ and ¼ of the wavelength in front of the model. After calibrating the probes at the zero point and setting the recording duration in the WVFW software, data collection was performed by activating the wave maker until the wave conditions stabilized. Once the wave graph was recorded, the machine was stopped, and the data was exported to '.xlsx' format, after which the entire process was repeated for each variation of the planned research parameters. The representation of the stages carried out in this study provides a clear picture of the research flow, from the initial stage to the final stage, as shown in Figure 5.

The initial stage of the literature study was conducted by collecting and analyzing relevant literature, including the characteristics of wave channels in producing waves with high variation and period, maximum channel capacity, and relevant laboratory data collection methods. This literature study aims to establish the theoretical basis and analysis methods to be used. Based on the results of the literature review, a physical model of a pyramid-shaped gabion wave breaker was designed, including its dimensions, constituent materials, and structural slope. The selection of the model's size and geometry referred to the suitability of the test scale in the laboratory wave channel. The designed model was tested in a wave channel to obtain data on the structure's response to various wave conditions. The testing was supplemented with additional simulations (if necessary) to support the validation of the physical test results. Prior to data collection, all measuring instruments were calibrated to ensure accuracy. The calibration process included wave height sensors, depth gauges, and data loggers.

Measurements were taken for wave parameters: Period (T), height (H), and water depth (d); gabion parameters: Material density (ρ_s), gabion weight (W), and gravitational force (g); fluid parameters: Water density (ρ_w); Structure geometry parameters: Structure height (h), Slope (θ = 1:1.5 and 1:2). The measurement data was processed to obtain the following input data: H_{max}, H_{min}, H_i, T, d, H_r, H_t. The computational procedure involves determining the incident wave height (H_i) and wavelength (L), followed by an assessment of the armor damage percentage. Furthermore, the analysis quantifies the stability coefficient (K_D) and the coefficients for wave reflection (K_r), transmission (K_t), and dissipation (K_d).

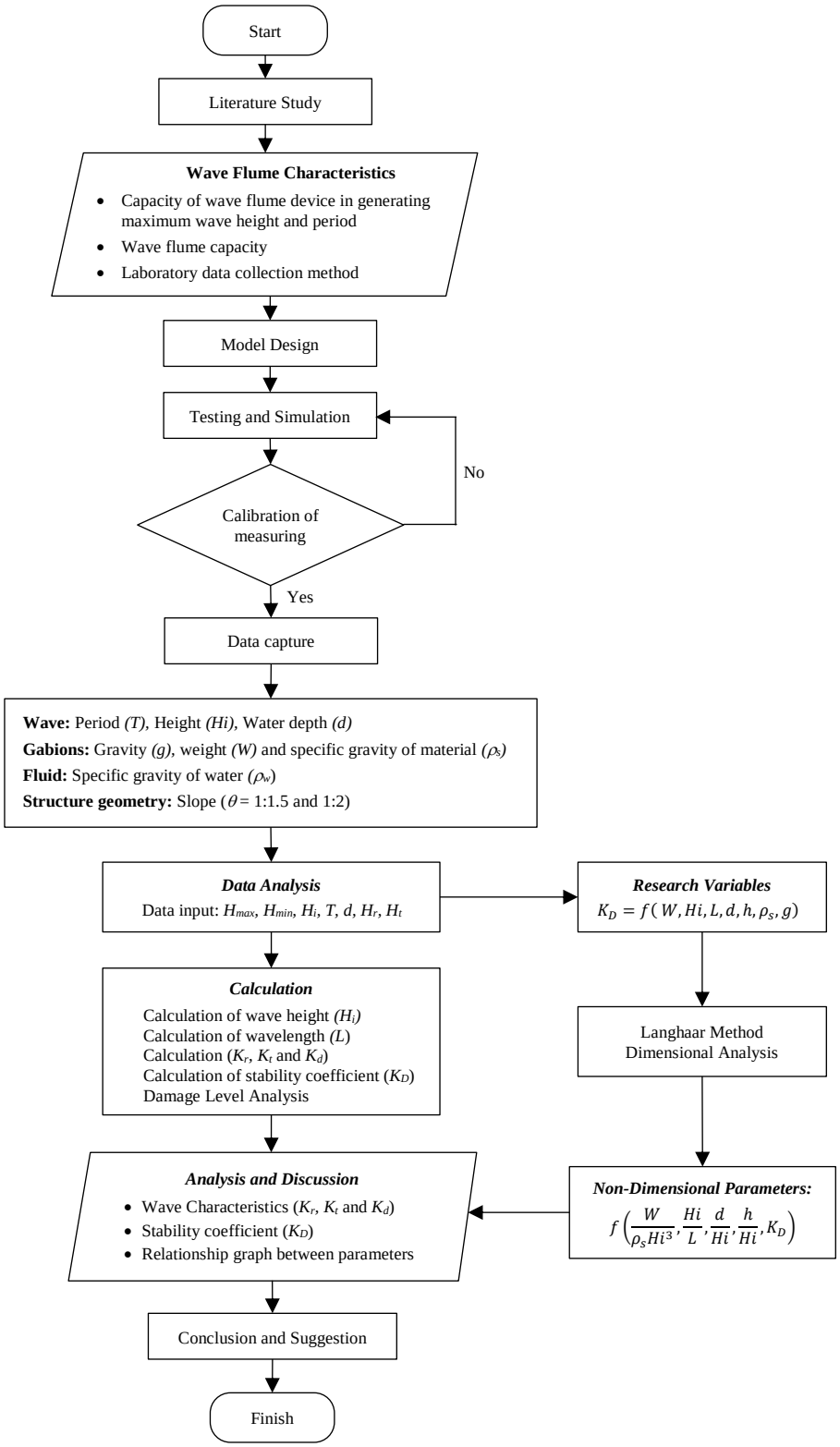

Figure 5. Flow chart of the research process

3.9. Langhaar Method Dimensional Analysis

Dimensional analysis simplifies relationships between physical variables using dimensionless parameters. The Langhaar Method is applied in this study due to its systematic and effective procedure for handling a given number of variables. The main principle of this method is to transform n physical parameters that have m basic dimensions (Mass [M], Length [L], and Time [T]) into a number of (n - m) dimensionless products (π). Mathematically, the dimensionless product π_j is expressed as a combination of the powers of physical parameters P_i:

$$\pi_j = P_1^{k1} P_2^{k2} P_3^{k3} \dots\dots\dots P_n^{kn} \quad (16)$$

If each parameter P_i has dimensions $M^{\alpha 1}L^{\beta 1}\ T^{\tau 1}$, then the condition for π_j to be dimensionless is the fulfillment of the following system of homogeneous linear equations for the exponents x_i.

$$\alpha 1K1 + \alpha 2K2 + \cdots \alpha nKn = 0 \quad (17)$$

$$\beta 1K1 + \beta 2K2 + \cdots \beta nKn = 0 \quad (18)$$

$$\tau 1K1 + \tau 2K2 + \cdots \tau nKn = 0 \quad (19)$$

The solution to this system of equations produces a coefficient matrix that determines the exponent value for each variable in the dimensionless group. In this study, the analysis is determined based on the main variables that affect the stability of the structure. The initial hypothesis regarding the influential variables is stated in the functional relationship in Equation 20:

$$K_D = f(W, Hi, L, d, h,\ \rho_s, g) \quad (20)$$

where, W is the weight of the pyramid-shaped gabion breakwater, H_i is the wave height, L is the wavelength, d is the water depth, h is the gabion height, K_D is the stability coefficient, ρ_s is the mass density of the material, and g is the acceleration due to gravity. Through the Langhaar analysis procedure, the following relationship between non-dimensional parameters is obtained:

$$f\left(\frac{W}{\rho_s Hi^3}, \frac{Hi}{L}, \frac{d}{Hi}, \frac{h}{Hi}, K_D\right) \quad (21)$$

Dimensional analysis yielded $f\left(\frac{W}{\rho_s Hi^3}, \frac{Hi}{L}, \frac{d}{Hi}, \frac{h}{Hi}, K_D\right)$, which were analyzed to evaluate the stability coefficient (K_D) and generate dimensionless parameter relationship graphs. The final stage involves drawing conclusions based on the test and analysis results, accompanied by recommendations for further research related to the design and optimization of the stability of pyramid-shaped gabion wave breakers. It should be noted that the influence of $\frac{\rho_w}{\rho_s} - 1 = \frac{\rho_s - \rho_w}{\rho_w} = \Delta$ is the relative density, and the slope of the structure (θ) as well as the unit weight of the gabion (W) are already accommodated in the stability coefficient (K_D), where $K_D = \frac{\gamma_r H^3}{W\left(\frac{\gamma_r}{\gamma_a} - 1\right)^3 Cot\theta}$.

4. Results and Discussions

4.1. Key Variables Affecting the Stability of Pyramid-Shaped Gabion Wave Barrier Protection Layers

According to the Hudson equation, the stability coefficient *(K_D)* is influenced by four main variables: wave characteristics, breakwater armor properties, fluid properties, and structural geometry. Wave-related variables include the wave period, wave height, and water depth, as well as the interlocking coefficient between gabions. The breakwater armor variables consist of gravity, gabion weight, and material specific gravity. The fluid variable is represented by the specific gravity of water, while the structural geometry variable is determined by the slope of the structure. A gabion breakwater functions to protect the coast by dissipating ocean wave energy, and its stability is strongly affected by the interaction of waves, fluid properties, and geometry. The Hudson equation thus serves as a key reference in the structural design, with the analysis conducted based on these primary influencing variables. This hypothesis is expressed mathematically, as shown in Equation 22.

$$K_D = f\left(\frac{Hi}{L}, \frac{d}{h}\right) \quad (22)$$

The functional relationship obtained (K_D) is the gabion stability coefficient, which determines the stability of the pyramid-shaped gabion protective armor. *(H_i/L)* is the wave steepness, a ratio related to wave characteristics; the steeper the value, the greater the loading effect the waves can cause. *d/h* is the ratio of water depth to structure height. This indicates seabed conditions and affects the dynamic pressure received by the structure. K_D is the structure stability coefficient, which describes how stable the structure arrangement is against waves based on *interlocking* and unit mass. Dimensional analysis helps simplify the complex relationships between variables, and nondimensional equations permit the generalization of structural design with key variables such as relative wave height, depth, and stability.

4.2. Influence of the Relationship Between Variables Affecting the Stability of Pyramid-Shaped Gabion Breakwaters

The influence of the relationship between variables that play a role in the stability of pyramid-shaped gabion breakwaters is to understand the mechanism of dynamic interaction between wave characteristics and the response of the structure to hydrodynamic loads, so that it can be used to assess the hydrodynamic performance of the structure, which is an overall assessment of how efficient the structure is. Optimizing the physical design of gabions through the analysis of variable relationships helps identify the most effective design parameters, such as structural slope, gabion

size, and shape (which influence porosity and damping capacity), as well as the configuration of the protection layer, all of which affect structural stability under varying wave conditions. Long-term stability forecasting is also essential, as the durability of gabion structures depends heavily on the accumulated cyclic wave loads. Understanding the relationships among these variables enables the estimation of stone unit displacement, the risk of scouring at the structure's toe, and potential volume loss caused by wave action or seepage. Furthermore, analyzing these variable relationships provides an empirical foundation for numerical and simulation models, offering valuable data for model validation, parameter calibration in design software, and adjustments under extreme climate scenarios. Ultimately, this understanding supports engineering and economic decision-making by improving material cost efficiency (e.g., stone size and gabion mesh selection), enhancing coastal protection efficiency, and assessing the risk of structural damage from extreme wave events.

4.2.1. The Effect of Wave Steepness (H_i/L) on the Percentage of Damage to Pyramid-Shaped Gabion Protection Layers

The effect of the relationship between wave steepness (Hi/L) and the percentage of damage to pyramid-shaped gabion protection layers for variations in slope and number of layers in pyramid-shaped gabion protection structures. Figure 6 shows a graph of four test variations, differing in the number of layers and structural slope (1:1.5 and 1:2). Overall, there is a strong positive correlation: as the wave steepness (Hi/L) value increases, the percentage of structural damage also increases. This is evident from the power regression curve (R^2 = 0.81–0.87).

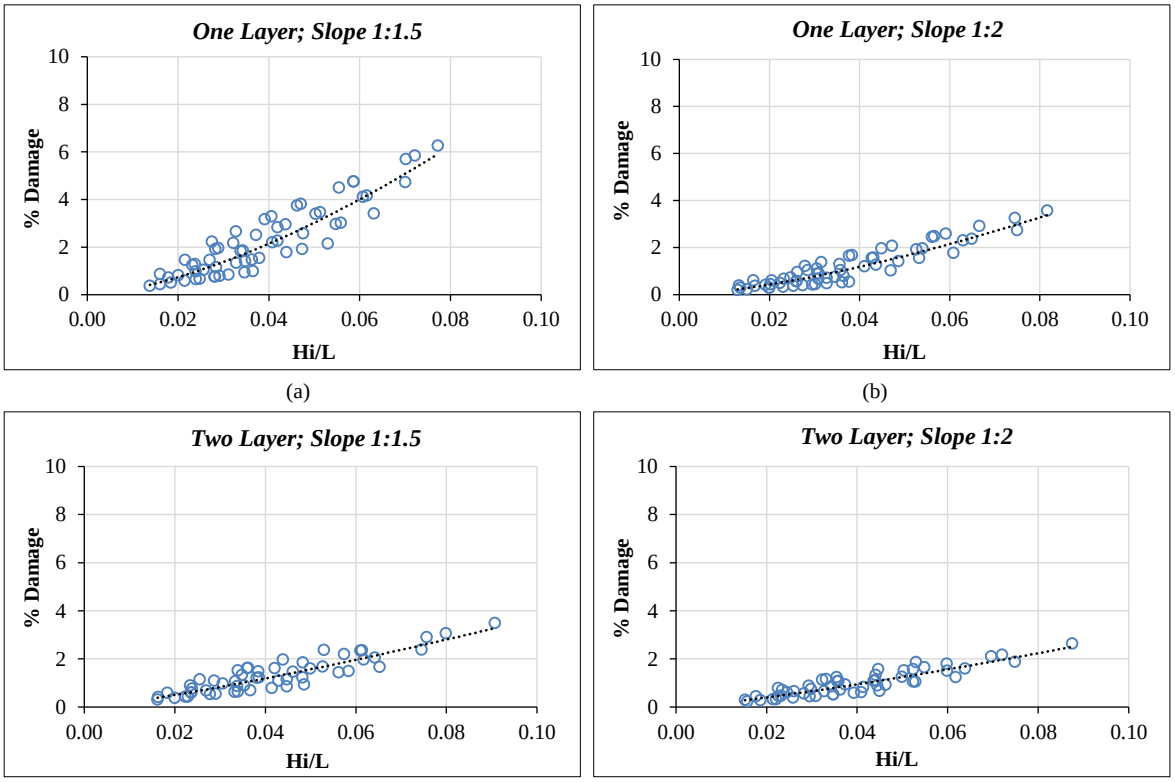

Figure 6. Relationship between wave steepness (Hi/L) and the percentage of damage to the pyramid-shaped gabion protective layer at varying slopes and gabion layers

Based on the experimental results shown in Figure 6, the analysis of the 1% damage criterion reveals that gabion stability is significantly governed by the number of armor layers and the structural slope. In the single-layer configuration, the 1% damage threshold occurs at relatively low wave steepness (H_i/L) values, specifically between 0.020 and 0.025 for a 1:1.5 slope, and slightly increasing to 0.030–0.035 for a 1:2 slope. Conversely, the double-layer model exhibits superior resistance, with the 1% damage limit reached only at higher wave steepness values of 0.035–0.040 for a 1:1.5 slope, and peaking at 0.045–0.050 for a 1:2 slope. These findings indicate that a double-layer arrangement combined with a gentler slope (1:2) provides optimal protection by effectively dissipating greater wave energy before the onset of initial damage.

Furthermore, at a maximum wave steepness of H_i/L = 0.06, the double-layer configuration with a 1:2 slope proved most effective, maintaining damage levels below 2%. In contrast, the single-layer model with a steep slope (1:1.5) demonstrated the highest vulnerability, with damage levels exceeding twice those observed in the double-layer configuration.

The 1:1.5 slope has a higher damage rate. In the graph (Figure 6a), the maximum damage in the one-layer variation reaches above 6%. The 1:2 slope variation shows a lower damage rate compared to 1:1.5. In the graph (Figure 6b), the maximum damage in the one-layer variation with a 1:2 slope is below 4%. A gentler slope dissipates wave energy more gradually, enhancing material stability. The effect of wave steepness (*Hi/L*) on the structural response in this study shows a pattern consistent with the phenomenon in the Overtopping Wave Energy Converter (OWEC) model. As stated by Puspita et al. [18], low wave steepness results in a larger relative wave run-up value. In the context of pyramid gabion stability, this condition is related to a longer duration of wave impact on the slope, while high steepness triggers kinetic collisions that increase the damage percentage to 6% under submerged conditions.

The effect of the number of layers on the one-layer variation is evident, as indicated by the steeper curve, which indicates a faster damage rate. The two-layer variation provides significant protection. In the graph (Figures 6c and 6d), the damage percentage is suppressed to below 4%, even for the same wave conditions as those of the one-layer variation. The addition of layers increases the interlock between gabion units and thickens the protection against wave energy penetration into the structure.

The increase in the percentage of damage, along with the increase in the *Hi/L* value in this study, is in line with the findings of Van der Meer [10], which states that the type of wave breaking, which is influenced by steepness, greatly determines the stability of the armor unit. The effectiveness of using two layers of gabion, which is more stable than one layer, confirms the principle of CERC [13] in the Shore Protection Manual, where the thickness of the protective layer (*n*) proportionally increases the resistance factor to lift force and drag force caused by wave impact.

4.2.2. The Effect of Relative Depth (d/h) on the Percentage of Damage to Pyramid-Shaped Gabion Protection Layers

The effect of the relationship between relative depth (*d/h*) and the percentage of damage to pyramid-shaped gabion protective layers is presented in Figure 7. Graph showing the relationship between the ratio of water depth to structure height (*d/h*) and the percentage of damage (% damage). There is a positive correlation between relative depth and the level of damage. As the *d/h* ratio increases, the percentage of damage tends to increase. This indicates that in deeper water conditions (relative to the height of the structure), the hydrodynamic forces acting on the gabion unit are greater

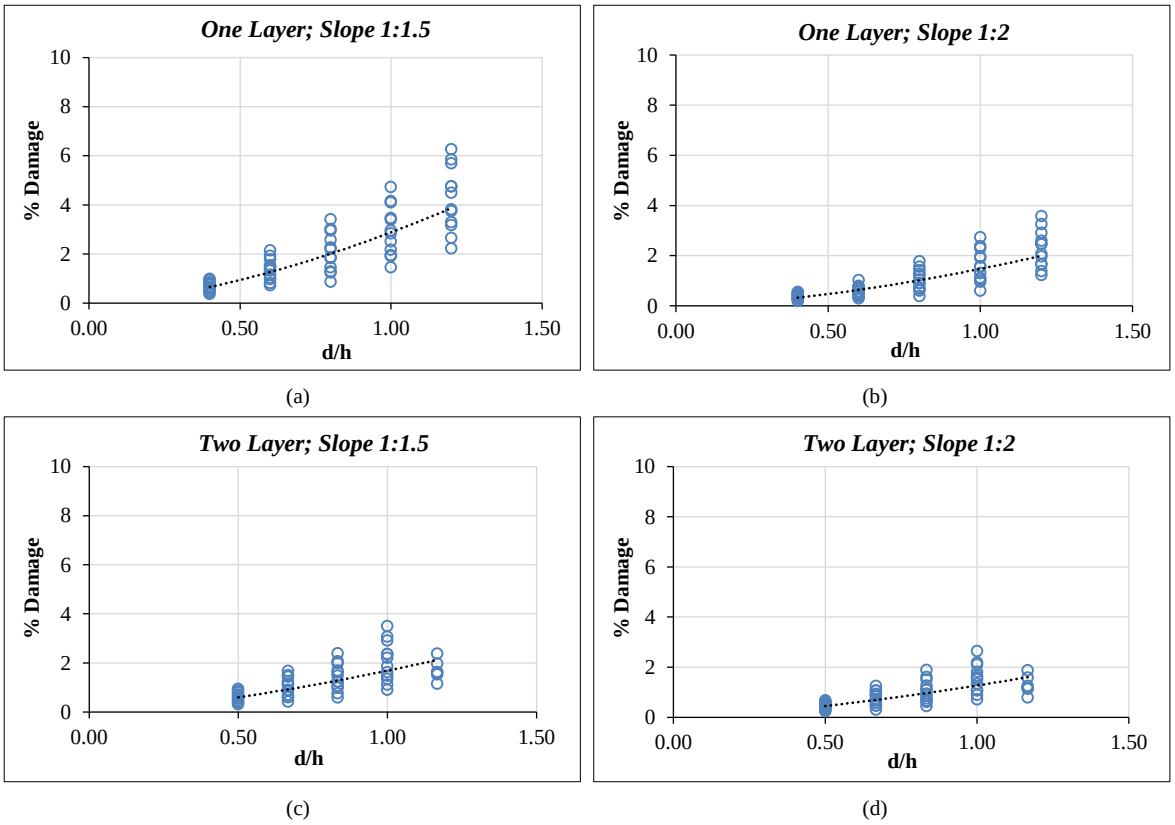

Figure 7. Relationship between relative depth (*d/h*) and percentage of damage to pyramid-shaped gabion revetment

Increasing the number of layers from one (Figures 7-a and 7-b) to two (Figures 7-c and 7-d) significantly improves stability, with single-layer configurations exhibiting a maximum damage value of 6% at a 1:1.5 slope. Damage is suppressed to below 4%, even at the highest *d/h* value. The effect of the structure slope, with a slope of 1:2, consistently shows a lower percentage of damage compared to a slope of 1:1.5, because a gentler slope is able to absorb wave energy more effectively through the *wave run-up* process.

The tendency for damage to increase with relative depth (*d/h*) in Figure 7 confirms Sorensen's theory [19] that in deeper waters, wave energy is not dissipated by friction with the seabed, causing it to strike structures with greater lift and drag forces. The phenomenon of higher stability at a slope of 1:2 compared to 1:1.5 is consistent with Hudson [9], where the unit weight of the protective layer required is inversely proportional to the slope function ($\cos\theta$ and $\sin\theta$), meaning that a gentle slope mechanically increases the safety factor against the overturning force of the gabion unit.

Analysis of the stability of pyramid gabion structures under three different hydrodynamic conditions: emerged, low crested, and submerged. Determining these conditions is crucial because the damage mechanisms in each zone have different characteristics. Emerged condition ($d/h < 1$), in this $d/h = 0.50$ and $d/h = 0.75$ in Figure 7, the percentage of damage is at the lowest level (below 2%). Most of the structure is above the water surface, so that wave energy is mostly reflected or broken on the lower slope. Uplift forces do not act on the entire gabion unit, improving stability. Low crested (LC) condition with ($d/h = 1$), the graph shows a significant spike in damage when the ratio reaches 1, especially in the single-layer variation (Figures 7-a and 7-b). This is a critical condition where the water is right at the top of the structure. Waves tend to *break* just above the crest, causing maximum turbulence that can pull the gabion units backward. Submerged condition ($d/h > 1$), at a *d/h* point of around 1.20, the damage percentage reaches its highest peak, approaching 6%. When the structure is submerged, waves pass over the top of the structure (complete overtopping). The high velocity of water particles above the low structure creates a strong *drag force*, which can displace the gabion units from their position.

These results indicate that *submerged* conditions ($d/h > 1$) cause the most serious damage, which is consistent with the findings of Van Der Meer [20] that the stability of protective units decreases dramatically as the ratio of depth to structure height increases to the point where waves break directly over the crest. Furthermore, the phenomenon of better stability in *emerged* conditions ($d/h < 1$) supports *the* theory in *the rock manual* at [21, 22], which states that structures with high crests effectively reduce energy through *wave run-up*, in contrast to submerged structures that receive the full hydrodynamic load on their surface.

By examining the graph of the relationship between *d/h* and % damage (Figure 7), we can map the performance of the pyramid gabion structure as follows:

- Semen Gresik industrial standard (0.5%), this gabion structure is only able to meet this very strict standard in emerged conditions ($d/h = 0.50$) with the use of two layers. In conditions where $d/h > 0.75$, almost all variations exceed the 0.5% damage limit.
- The standard in this study is the stability of the protective layer of the pyramid-shaped gabion wave breaker (1%). This limit can still be met in emerged conditions with either one or two layers. In LC conditions ($d/h = 1$), the one-layer variation (Figures 7a and 7b) begins to fail to meet the standard because the average damage is above 1%.
- Van der Meer [10] s (2.5%) consistently meet this standard even under submerged conditions ($d/h = 1.20$). One-layer structures with a slope of 1:1.5 fail to meet this standard when waves become more extreme or the d/h ratio is high.
- CERC's [13] standard (5%), almost all variations except for the one-layer structure with a slope of 1:1.5 at a high *d/h* were below the 5% threshold. Pyramid gabions generally meet US coastal protection safety standards.

This analysis shows that the determination of structural failure is highly dependent on the threshold used. Test results show that in submerged conditions ($d/h = 1.20$), the use of a single layer of gabion protection has a high risk of failure because it exceeds the Jayewardene et al. [23] threshold of 2.5%, but is still within the safe limit of CERC [13], which allows damage of up to 5%. The durability of the two-layer structure, which remains below 2% damage even under submerged conditions, proves that this design is highly reliable, even when compared to the conservative standard of Semen Gresik (0.5%), which demands high stability for vital infrastructure. Based on the analysis in Figure 7 (*d/h* graph) and Table 5 comparing the safety status of the structures:

Table 5. Comparison of structural safety status

Damage Tolerance Standard	Threshold Value (%)	Emerged Condition Status ($d/h < 1$)	LC Condition Status ($d/h = 1$)	Submerged Condition Status ($d/h > 1$)
Gresik Cement	0.5%	Safe (Only 2 Layers)	Failed (Exceeding limit)	Failed (Exceeded limit)
This Research	1.0%	Safe	Critical (1 layer starting to fail)	Failure (Exceeding limits)
Van der Meer [10]	2.5%	Very Safe	Safe	Safe (Only 2 Layers)
CERC [13]	5.0%	Very Safe	Very Safe	Safe (Almost entirely)

The stability of the protective layer of pyramid-shaped gabion wave breakers is greatly influenced by wave steepness (H_i/L) and relative depth (*d/h*). The strongest correlation was found in the wave steepness parameter ($R^2 = 0.81 - 0.87$), indicating that the physical characteristics of the waves are more dominant in determining the rate of damage than the water depth ratio.

In terms of operational thresholds, the pyramid-shaped gabion wave breaker protective layer structure performed very well in emerged conditions ($d/h < 1$), where all variations met the standards of 2.5% for the Jayewardene et al. [23] and 5% for the CERC [13]. Under submerged conditions ($d/h = 1.20$), the damage rate increased to 6%, meaning the single-layer structure exceeded the international tolerance limit. The use of a Two-Layer system proved crucial to maintaining structural integrity below the 4% threshold under submerged conditions. To meet very strict industry standards such as Semen Gresik (0.5%), the design must focus on *emerged* conditions with a gentle slope (1:2) to reduce the lift and hydrodynamic drag forces that occur when the top of the structure begins to flood.

Looking at the trend in Figure 7, setting the limit at 1% provides a very clear design constraint, with a safe zone (emerged) at a d/h ratio < 1.0, and most data points below or very close to the 1% line. This proves that the pyramid-shaped gabion arrangement is highly effective in conditions where the structure emerges above the water surface. The critical zone (low crested) is observed when $d/h = 1.0$, with the graph showing many points beginning to exceed the 1% threshold. This standard accurately identifies the safe operational water level limit for the structure's low-crested zone. The failure zone (submerged) is observed under conditions where $d/h > 1.0$, with damage surging to 6%. The 1% standard helps draw a clear conclusion that this structure is not recommended for submerged conditions without additional reinforcement.

In coastal engineering, stricter standards (such as 1% compared to 5% of CERC) are used to minimize long-term maintenance costs. Minor damage detected early prevents catastrophic failure in the future. Gabion material differs from single stones in that gabions rely on the integrity of the wire. The 1% limit is crucial to prevent excessive wire deformation, which could dislodge fill stones. Setting a damage tolerance standard of 1% in this study is a conservative approach that aims to ensure the absolute stability of the pyramid gabion structure. Based on Figure 7, this standard successfully separates the performance of the structures significantly, where the *emerged* condition remains within safe limits, while the *submerged* condition exceeds these limits. This is in line with the principle of "Burcharth [24]" that innovative protective units require low damage thresholds to accommodate the uncertainty of hydrodynamic forces in the field.

4.2.3. Determination of Stability Coefficient (K_D) Based on Standard Damage Percentage

The determination of the stability coefficient (K_D) is based on the damage percentage standards illustrated in Figure 8. As a critical parameter in the Hudson formula, K_D dictates the resilience of armor units against wave forces. Figure 8 reveals a positive power law relationship with exceptionally high coefficients of determination (R^2), ranging from 0.898 to 0.928. These values indicate that K_D is directly proportional to damage tolerance; essentially, the pyramidal gabion units possess a stability reserve that increases as their shape adjusts or their interlocking tightens.

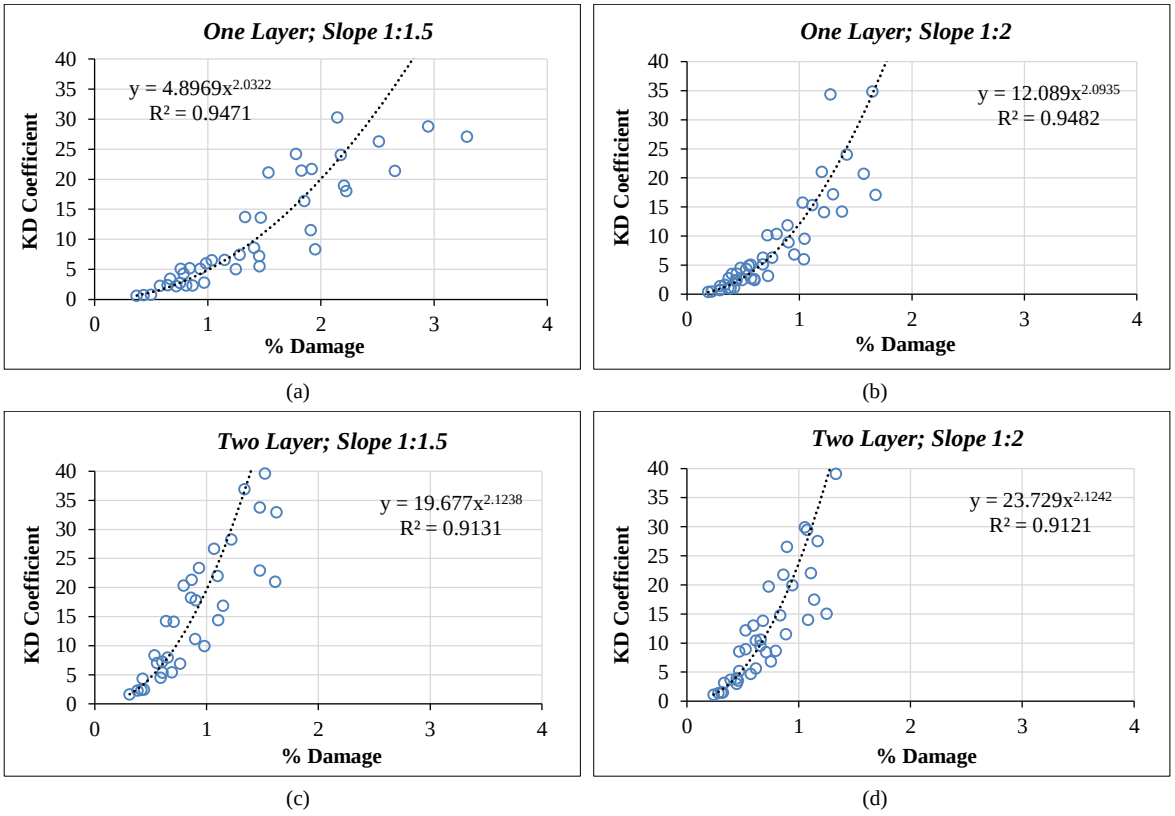

Figure 8. Relationship between damage percentage and stability coefficient (K_D) of pyramid-shaped gabion protective layers

Regarding the effect of layer thickness, the single-layer variations (Figures 8-a and 8-b) exhibit a broader damage range, exceeding 3% to reach specific K_D values. In contrast, the double-layer variations (Figures 8-c and 8-d) display significantly steeper curves. At minimal damage levels (approximately 1–1.5%), the K_D values surge drastically to the 35–40 range, demonstrating the superior stability provided by double-layer systems. Furthermore, gentler slopes (1:2) tend to yield higher K_D values compared to steeper gradients (1:1.5) at equivalent damage levels, suggesting that a milder geometry enhances the hydrodynamic efficiency of the pyramidal gabion units.

Theoretically, the value *of* K_D is influenced by the shape of the unit, the level of interlocking, and the surface roughness. The significant increase in the K_D value when using two layers of pyramid gabions, as shown in Figures 8-c and 8-d, is in line with the research [9] which states that the stability coefficient is highly dependent on the degree of interlocking between units, where the pyramid shape creates a larger contact area compared to ordinary natural stones. This phenomenon is also supported by the theory in the Shore Protection Manual [13], which explains that the K_D value for artificial armor units that have mechanical interlocking, such as pyramid gabions, will be much higher than crushed stone, allowing the structure to remain stable even when using lighter unit weights on the same slope.

Analysis based on the 1% damage standard, if using a 1% damage threshold in Figure 8-c (two layers, slope 1:1.5), when damage is 1%, the K_D value is in the range of 20.00. In Figure 8-d (two layers, slope 1:2), when damage is 1%, the K_D value increases to around 23.00. By setting a limit of 1%, pyramid gabions exhibit high stability due to the low standard K_D value (typically 2.0-4.0) of crushed stone. Table 6 below summarizes the stability coefficient (K_D) values calculated based on the regression equation in Figure 8 for a damage level of exactly 1%. These results strongly suggest that pyramid gabions outperform conventional armor units. Based on the equation $y = A\ x\ B$ (where y is K_D and x is % Damage) from Figure 8.

Table 6. Stability coefficient values (K_D)

Structural Variation	Regression Equation	K_D Value (1% Damage)	Stability Category
One layer; θ = 1:1.5	$K_D = 4.8969\ x^{2.0322}$	4.90	Moderate
One layer; θ = 1:2	$K_D = 12.089\ x^{2.0935}$	12.09	Height
Two layers; θ = 1:1.5	$K_D = 19.677\ x^{2.1238}$	19.68	Very High
Two layers; θ = 1:2	$K_D = 23.729\ x^{2.1242}$	23.73	Maximum

The K_D values obtained (4.90 to 23.73) indicate the mechanical superiority of the pyramid shape compared to standard protection units. Based on the analysis in Figure 8, at a 1% damage level, a two-layer pyramid gabion with a slope of 1:2 achieves a K_D value of 23.73, which far exceeds the K_D value *of*natural stone (K_D = 2.0) or Tetrapod (K_D = 7.0 - 8.0) as listed in CERC [13]. This high value confirms the theory [9] that geometric shapes that allow massive interlocking between units can significantly increase the stability of the structure. Consistent with research [10], the system's efficiency derives from the protective layer's thickness, which increases surface roughness and effectively reduces wave kinetic energy prior to unit displacement.

The experimental results show that the K_D value reached 23.73, which is significantly higher than that of conventional concrete units. This structural advantage is due to the internal friction between the graded stones in the gabion and the flexible nature of the wire mesh, which allows minor shifts that further tighten the interlocking between the pyramid units. The high R^2 value on the regression curve was obtained from three repetitions for the period (T) and stroke (S), and five repetitions for the flow depth (d) for each test condition, ensuring statistical reliability and minimizing experimental uncertainty.

This shows that gabions with materials that have a higher stability coefficient require a smaller relative volume and weight to achieve the same level of stability in withstanding waves. Consistent with Srineash & Murali [25], porosity reduces effective wave forces, and numerical optimization [26], demonstrates the efficiency of multi-layer designs. However, under extreme conditions, Van der Meer [10] argues that slope outweighs the number of layers, highlighting the importance of porous gabions over massive rock armor in this graph.

4.3. Wave-Structure Interaction Processes

The real-time hydrodynamic interactions between the incident waves and the armor units were documented to validate the stability analysis. Figure 9 provides visual evidence of these processes, illustrating the behavior of wave run-up, run-down, and the resulting overtopping on the pyramid-shaped gabion samples.

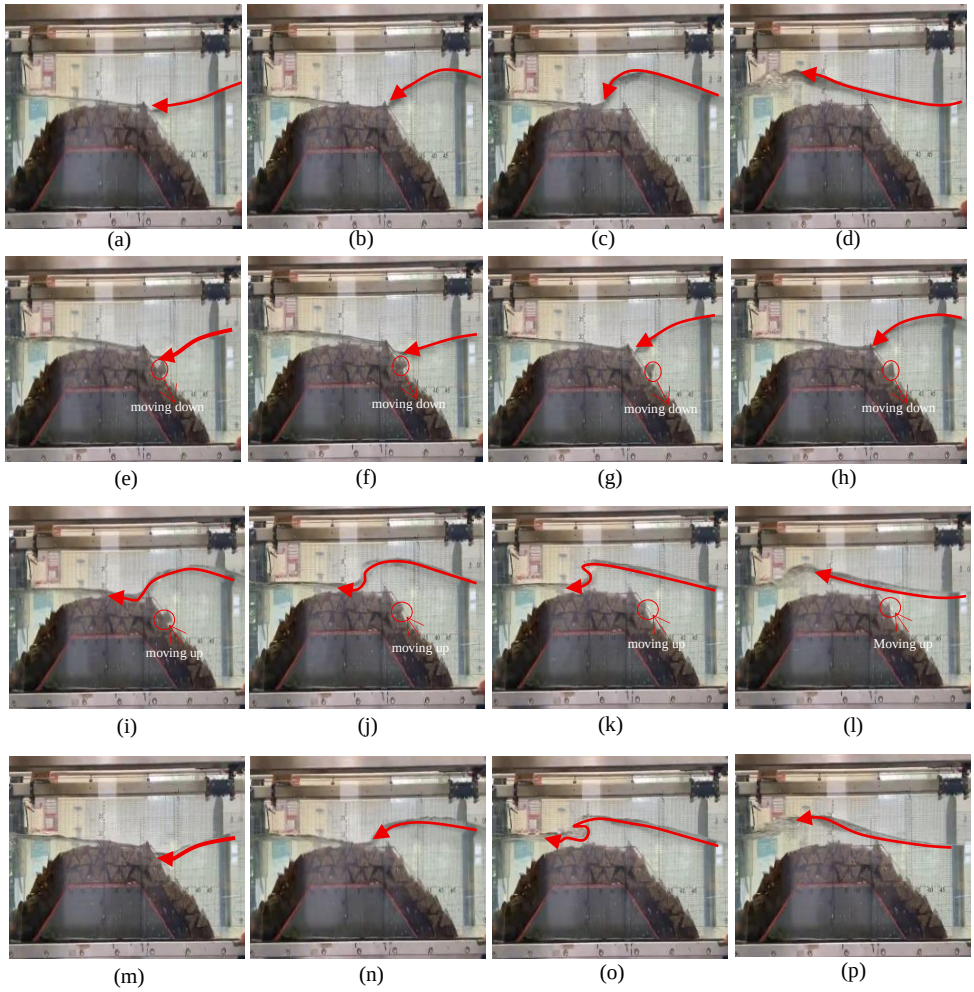

Figure 9. Visual documentation of hydrodynamic processes during laboratory testing: (a–d) wave run-up on the pyramid gabion slope; (e–h) wave run-down and energy dissipation; (m–o) significant overtopping during submerged conditions

During the run-up phase (Figures 9a–d), the energy is significantly attenuated by the structure's permeability and the interlocking geometry of the pyramids. In contrast, the submerged scenarios (Figures 9m–o) demonstrate significant overtopping, where the wave crest passes over the structure, exerting maximum drag and lift forces on the armor units. These visual observations correlate with the higher damage percentages recorded in the experimental data, particularly when the relative water depth exceeds the crest elevation ($d/h > 1.0$).

The experimental results show a strong correlation between the visual hydrodynamic process and the measured stability parameters. The stability of the pyramid-shaped gabion unit is greatly influenced by the wave slope (H_i/L) and relative water depth (d/h), which directly affect the magnitude of the force acting on the protective layer. As shown in the analysis, the maximum stability coefficient (K_D) reaches 23.73 under submerged conditions ($d/h < 1.0$). This very high value, compared to traditional concrete units, is theoretically justified by the high internal friction and mechanical interlocking provided by the pyramid geometry. The permeable nature of gabions allows for internal flow, which effectively reduces the pore pressure gradient and minimizes the uplift forces that typically compromise the stability of solid protective units. Conversely, under submerged conditions ($d/h > 1.0$), the K_D value decreases to a range of 4.9 to 8.3. This decrease is consistent with visual evidence of significant overflow shown in Figure 9. Under these conditions, the structure is exposed to intense friction and uplift forces as wave crests pass over the defense layer. Nevertheless, the maximum recorded damage level was only 6%, which is still within acceptable limits for flexible structures. Regression analysis yielded a high coefficient of determination (R^2), further confirming the empirical relationship between the stability coefficient and the hydrodynamic variables tested.

4.4. Stability Coefficient (K_D) Values for Gabion Pyramid-Shaped Wave-Breaking Protective Layers

The stability coefficient (K_D) values obtained from experimental studies on wave-breaking protective layers using pyramid-shaped gabions. The Hudson equation uses the stability coefficient (K_D) to determine the required weight of the protective armor layer against wave action. K_D varies depending on the structure's slope (θ), number of armor layers, and research conditions (emerged, low crested, and submerged).

- ***The influence of wave characteristics and relative depth***

Analysis reveals wave steepness (H_i/L) as the strongest predictor of damage to pyramid-shaped gabion protective layers, exhibiting a correlation of 0.87. An increase in the H_i/L value consistently increases the percentage of structural damage because greater wave kinetic energy hits the protective units. This is in line with the theory of Van der Meer [10], which states that the type of wave breaking, which is influenced by steepness, greatly determines the stability of the armor unit.

The ratio (d/h) defines three hydrodynamic performance zones for the structure. In emerged conditions ($d/h < 1$), the structure exhibits the highest stability with damage below 1%. However, in submerged conditions ($d/h > 1$), damage increases to 6% due to the drag force and uplift force acting fully on the entire surface of the gabion unit. This condition confirmsSorensen's [19] finding that in deeper waters, wave energy is not dissipated by friction with the seabed, causing it to hit the structure with greater force.

- ***Evaluation of the stability coefficient (K_D) at the 1% threshold damage***

To ensure long-term safety, this study sets a damage threshold of 1%. This limit is more conservative than the 5% standard set by CERC [13] or the 2.5% standard set by Van der Meer [10], but it is highly relevant for maintaining the integrity of gabion wire mesh against progressive deformation. Based on the calculation results at the 1% threshold, the stability coefficient (K_D) of the pyramid gabion shows exceptional performance: the two-layer structure at a slope of 1:2 achieves a maximum K_D value of 23.73, while the two-layer structure at a slope of 1:1.5 achieves a K_D value of 19.68. These K_D values far exceed the standard values for conventional armor units, such as Tetrapod K_D around 8, or crushed stone K_D ranging from 4 [11, 13]. The high K_D value confirms the theory [9] that geometric shapes that allow massive interlocking between units, such as pyramidal shapes, can significantly increase the stability of the structure against wave impact forces. Standard K_D values for gabions are rarely published in standard manuals such as *the Shore Protection Manual* (SPM) or EurOtop, because gabions are often analyzed as *monolithic structures* whose failure involves sliding or overturning [27]. Table 7 outlines the model's strengths and weaknesses, supported by experimental data.

Table 7. Model advantages and limitations with experimental data support

Aspect	Advantages	Limitations
Hydrodynamic Performance	• The dissipation coefficient (K_d) averaged > 0.80 at slopes of 1:2 and 1:1.5, indicating high wave energy absorption capacity. • Average reflection coefficient (K_r) <0.15, indicating low back pressure on incoming waves.	• The dissipation effectiveness decreased by ±12-15% when the gabion pores were filled with sediment (here are the partial clogging simulation results). • At extreme waves (Hi > 0.18 m in the scale model), Kd decreased to 0.58, requiring additional reinforcement of the protection layer.
Construction and Materials	• The use of locally available 10–15 cm crushed stone reduced material costs by approximately 20% compared to molded concrete units. • The modular structure enables manual assembly without the need for a crane, thereby accelerating construction time by about 25%.	• Deformation of the protection layer may occur if the size of stones in the gabion varies too much (>25% difference). • Immersion tests show the galvanized steel wire begins to show significant corrosion after 6-8 months without additional protection.

The stability coefficient (K_D) from the results obtained indicates that the selection of the structure's slope has a dominant influence on stability compared to the number of layers, but the number of layers remains important for maintaining the long-term performance of the structure. These results are in line with Van der Meer [10] which shows that a gentle slope increases the stability of the armor unit, as well as [9] which confirms the positive relationship between a gentle slope and an increase *in* (K_D). Srineash et al. [25] study on porous reef *breakwater gabions* also found that double-layer configurations and gentle slopes significantly reduce damage levels and improve stability. Eldrup et al. [28] highlights that permeable structures with gentler slopes sustain higher (K_D) values despite increasing wave steepness.

Several studies examining protective layers have shown that the stability coefficient (K_D) of pyramid-shaped gabion wave breakers is influenced by the unit weight of the gabion, wave parameters (height, period, and steepness), and the geometric configuration of the structure. Consistent with Srineash & Murali [25], these results emphasize that the hydrodynamic resistance of gabion-based breakwaters depends on the proper calibration of unit weight against prevailing wave conditions.

Compared to conventional rock-based or Accropode wave breakers, pyramid-shaped gabion structures offer advantages in energy dissipation due to their porosity, thereby reducing wave pressure behind the structure. These results are consistent with the findings of Bai et al. [29], which show that the reflection coefficient (K_r) can be suppressed in porous structures, although differences in relative depth and wave breaking intensity still affect performance.

In terms of multi-purpose functionality, Scheel [30] reported that gabion walls can be used not only for coastal protection but also for applications such as fish farming or current control. In the context of pyramidal shapes, this configuration provides additional stability through a wide-based geometry that reduces shear forces; the K_D value tends to be higher than that of vertical or upright gabions. Vieira et al. [31] emphasized the importance of considering the distance between structures in coastal defense design because it affects current patterns and sediment dynamics. In pyramid-shaped gabion models, the spacing and layout of the modules can be optimized to minimize erosion behind the structure, thereby improving its long-term performance.

Compared to previous research on protective layers, the proposed design offers several distinct advantages: superior energy dissipation due to high porosity, enhanced structural stability through its pyramidal geometry, and socio-economic added value via its multi-purpose functionality. Limitations: K_D performance remains sensitive to relative depth and wave steepness; it requires optimal spacing to avoid local turbulence effects. These findings reinforce the idea that pyramid-shaped gabion designs can be an effective alternative to wave breakers in shallow waters, with competitive performance compared to conventional structures if their placement and dimensions are optimized according to local wave conditions.

4.5. Wave Deformation Through the Weight of Pyramid-Shaped Gabion Protection Layers

The relationship between wave steepness (H_i/L) and reflection coefficient (K_r), transmission coefficient (K_t), and dissipation coefficient (K_d) for variations in slope and number of layers in the pyramid-shaped gabion protective structure is presented in the graphs in Figures 10 and 11. Based on the graph in Figure 10, we can identify several patterns of wave behavior when interacting with the structure, with the dissipation coefficient (K_d) showing dominance in emerged conditions. This indicates that the pyramid gabion structure is very effective in absorbing wave energy through internal friction within the gabion pores. The transmission coefficient (K_t) appears to increase significantly in *submerged* conditions. This is logical because waves can pass over the top of the structure (overtopping) more easily. The reflection coefficient (K_r) tends to be low and stable (> 0.30). This proves that the pyramid shape and porous gabion material are able to minimize wave reflection that can cause erosion at the foot of the structure (scouring).

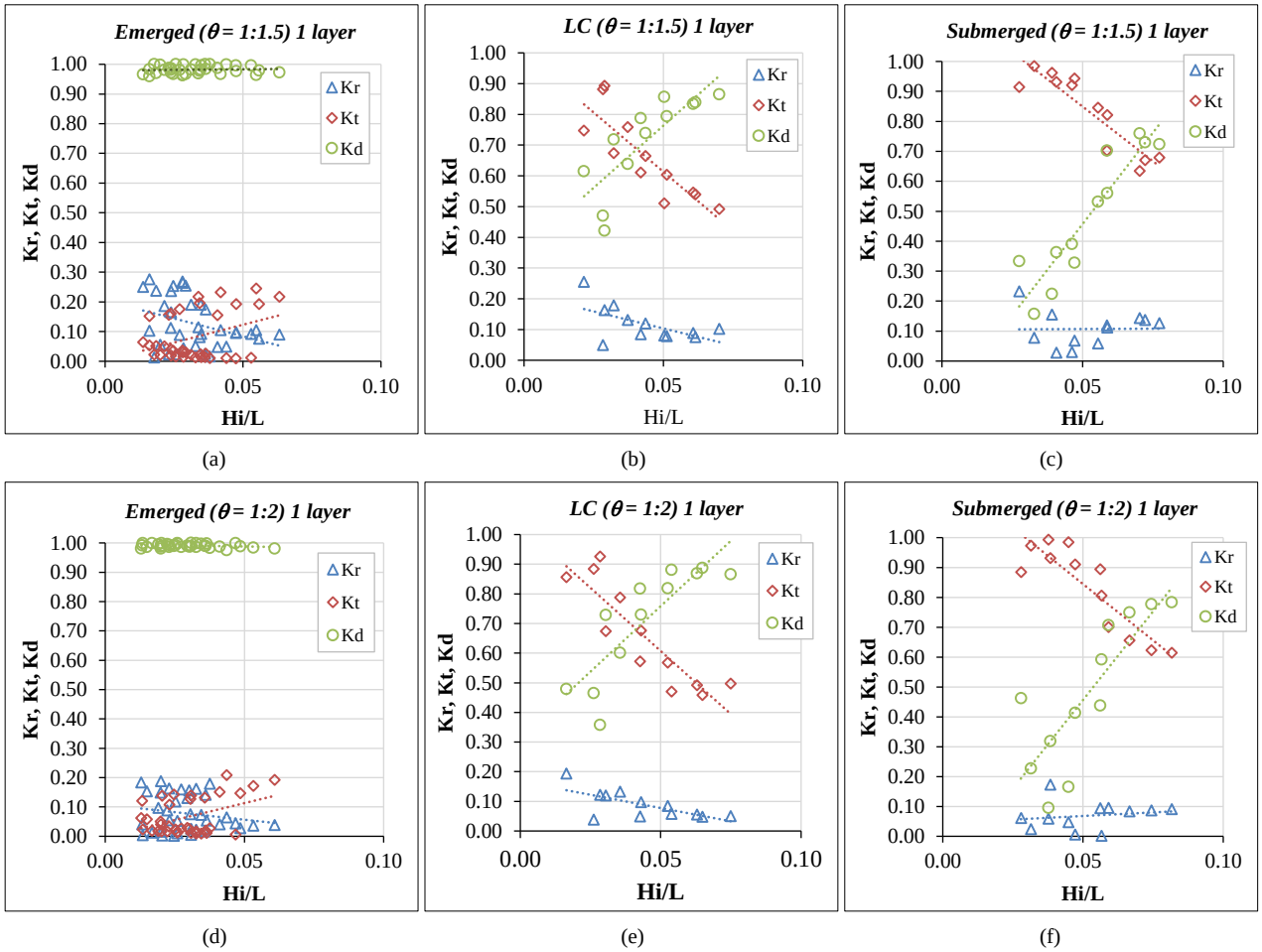

Figure 10. Relationship between wave steepness *(Hi/L)* and reflection coefficient (K_r), transmission coefficient (K_t), and dissipation coefficient (K_d) for variations in slope and conditions of a single layer of pyramid-shaped gabions

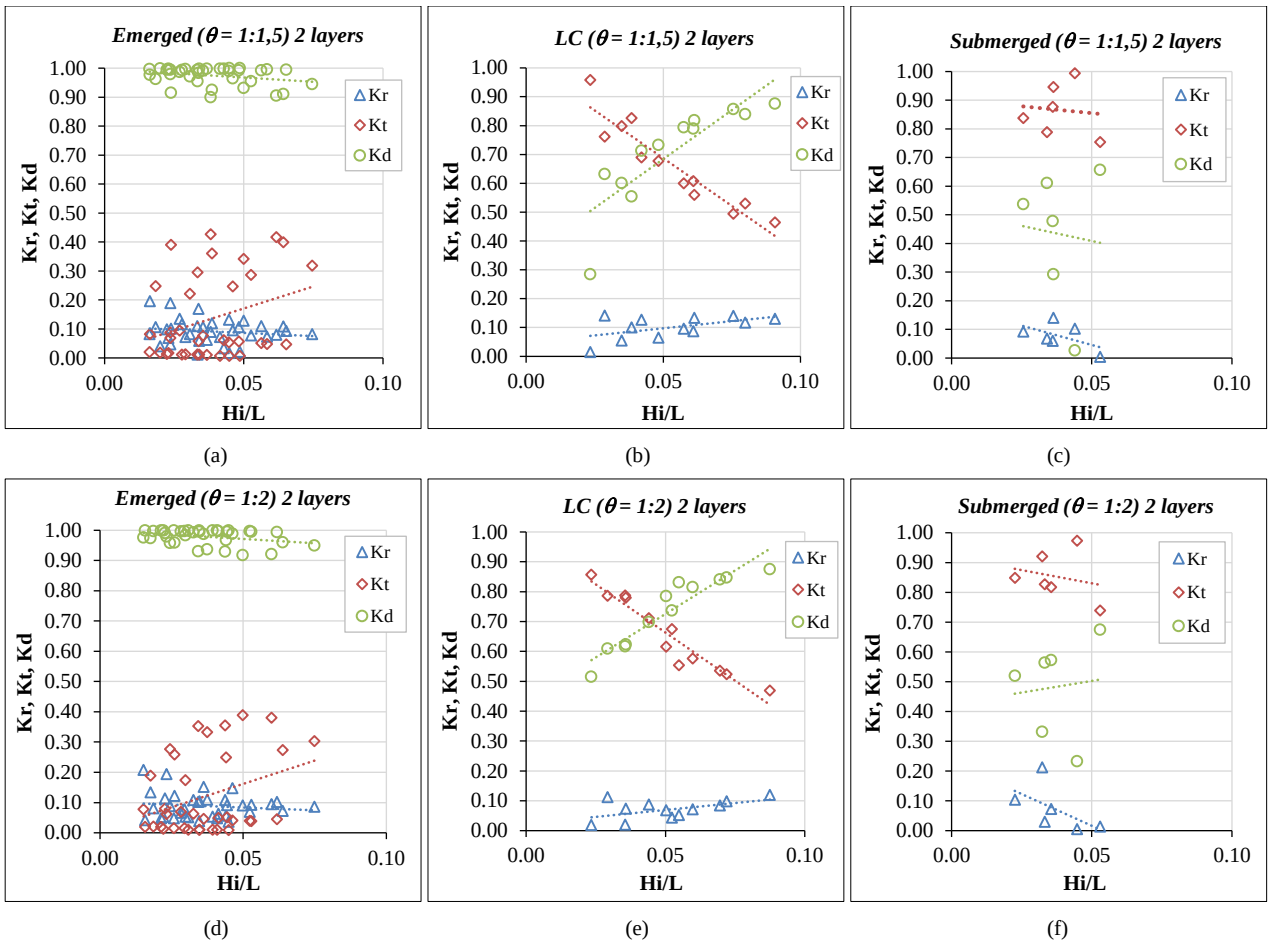

Figure 11. Relationship between wave steepness *(H_i/L)* and reflection coefficient *(K_r)*, transmission coefficient (K_t), and dissipation coefficient (K_d) for variations in slope and conditions of 2-layer gabion s in pyramid shape

Theoretically, wave interaction with porous structures follows the law of energy conservation: $K_r^2 + K_t^2 + K_d^2 = 1$. The relationship between *Hi/L* and *Kt* and *Kr* from the results of Figure 10 shows that the greater the wave steepness (*Hi/L*), the *Kt* value tends to decrease while *Kd* increases. This phenomenon aligns with Thesnaar [32] which suggests that steeper waves tend to break prematurely upon impacting porous structures, thereby reducing the energy transmission. The pyramid-shaped gabions yield a higher dissipation coefficient (K_d) compared to rigid, massive concrete structures. This is further supported by Jafari et al. [33], which attributes this to the internal turbulence created within porous materials, effectively converting wave kinetic energy into heat or dissipated energy.

Based on the graph in Figure 11 for slope variations θ = 1:1.5 and θ = 1:2 with two layers, the dissipation coefficient (K_d) dominates in the *emerged* condition, with K_d values in the very high range (approaching 1.00). The use of two layers increases the cavity volume within the structure, allowing wave energy to be absorbed more effectively through internal turbulence within the gabion. The behavior *of the* transmission coefficient (K_t) under *low-crested* (LC) and *submerged* conditions shows a decreasing trend as wave steepness (H_i/L) increases. This is because steeper waves tend to break earlier when they hit the structure. Compared to the single-layer data in Figure 11, the use of two layers visually suppresses the K_t value lower in *low-crested* (LC) conditions, which means that the structure is more effective at reducing the transmission wave height. The reflection coefficient (K_r) shows a consistently low reflection value (generally < 0.20). This indicates that the pyramid shape, combined with the surface roughness of the two layers of gabion, is very effective in breaking wave energy rather than reflecting it back towards the sea.

The addition of layers to porous coastal protection structures aims to increase the surface roughness index and pore volume. According to the theory of energy dissipation in porous media, the addition of layers increases the length of the water path within the structure. This aligns with Chwang & Chan [34], which demonstrates that layered coastal protection structures enhance the dissipation coefficient by increasing friction between the fluid and the gabion units. Figure 11 shows that K_t is inversely proportional to H_i/L. Theoretically, waves with high steepness have more unstable energy, making them easier to dissipate by porous structures. This is supported by Thesnaar [32], who, in a similar experiment, found that wave steepness is a major determining factor in the effectiveness of wave breakers.

Overall, increasing the number of layers from one to two significantly enhances the structure's capacity to dissipate wave energy (K_d) and reduce transmission (K_t). For the one-layer configuration in emerged conditions, K_d remains stable

between 0.95 and 0.98. In contrast, the two-layer configuration shows a consistent increase in K_d, approaching 1.00. This improvement is attributed to increased surface roughness and cavity volume, which allow the structure to absorb nearly all incident wave energy. This pattern indicates the phenomenon *of energy bypass* or wave penetration through the pores of a permeable structure [35]. In the *submerged* condition, the single-layer variation *of* K_t reaches high values of 0.90–1.00, while the double-layer variation in the *submerged* condition shows a slightly lower and more stable trend *of* K_t at with high slopes. The 2-layer structure is more effective in inhibiting water flow over the structure (*overtopping*) due to its thicker physical barrier. This trend is consistent with the findings of Rageh & Koraim [36], which show an increase in wave attenuation with the addition of layers and a more gentle slope arrangement. The variation in the single-layer reflection coefficient (K_r) is in the range of 0.10 - 0.25, while the variation in the two-layer is lower, with values below 0.15 in *emerged* conditions. The two-layer gabion is more absorptive than reflective compared to the single layer. This phenomenon is supported by the theory that steeper waves are more easily penetrated by permeable structures than reflected [37].

The addition of a gabion layer theoretically increases the porosity and surface roughness. According to Chwang & Chan [34], thicker coastal protection structures create greater turbulence within the material voids, which directly increases the K_d value and decreases K_t. In Figures 10 and 11, it can be seen that as the wave steepness (H_i/L) increases, the K_t value decreases. This shows that pyramid gabion structures (both single and double layers) are very effective as breaking wave breakers. The pyramid/pyramid geometry forces the waves to break earlier, and this effect is amplified in double-layer structures due to the more dominant elevation and thickness of the structure. These results reinforce the recommendation to use permeable, tiered, and sloping structures for extreme wave attenuation in coastal areas [38, 39]. In line with the development of hybrid wave-breaking structures such as *oscillating water columns* that utilize slopes of 45° to 60° to optimize internal pressure and stability, the use of pyramid-shaped gabions in this study also shows that unit geometry is crucial in determining the efficiency of the structure [40, 41]. Table 8 compares the pyramid-shaped gabion models with existing research, focusing on the coefficients K_r, K_t, and K_d, along with their respective design mechanisms.

Table 8. Comparison of the pyramid-shape gabion model with relevant research

Topic	Model research findings (Gabion pyramid)	Relevant research findings	Red thread	Topic
Reflection (K_r)	Low: Range 0.10–0.25 (1 layer) and < 0.15 (2 layers) at a ratio of 1:2–1:1.5 with low back pressure	Porous and submerged structure: K_r decreases as pores become effective, depending on *d/L* and *B/L*; K_r tends to be maximum at *B/L* around 0.2-0.25 and then decreases as *B/L* increases [42-44].	The low performance of the pyramid-shaped gabion model is consistent with the trend of porous or submerged structures: porosity with 'elongated flow paths' suppresses reflection.	Reflection (K_r)
Transmission (K_t)	Moderate to low (implied from high K_d)	Kt decreases as relative depth *(d/L)* increases and as the width or effective layer of the structure increases; the K_t *(d/L)* relation is clear in the submerged or perforated model [43, 45].	If the field location has a larger *d/L* (shorter waves or deeper water), the K_t of the pyramid-shaped gabion model has the potential to decrease further.	Transmission (K_t)
Dissipation (K_d)	High: K_d emerged stable at 0.95–0.98 (1 layer) and consistently approaches 1 (2 layers)	In porous or permeable structures, high K_d is achieved when K_t and K_r are both moderate; theoretical $K_d = \sqrt{(1 - K_t^2 - K_r^2)}$ is widely used for evaluation [46].	The K_d value of the pyramid-shaped gabion model falls within the 'good' range for porous breakwaters, aligning with the K_t–K_r–K_d evaluation framework.	Dissipation (K_d)

4.6. Discussion and Comparative Analysis

The experimental results demonstrate that pyramid-shaped gabion units possess a high degree of hydraulic stability, as evidenced by their stability coefficient (K_D) values. This stability is closely linked to the energy dissipation mechanisms inherent in permeable structures. Unlike smooth, impermeable armor units that reflect a significant portion of wave energy, the porous nature of gabions allows waves to penetrate the armor layer. This internal flow induces turbulence among the stone fillers, effectively dissipating wave energy and reducing the back-pressure that typically contributes to unit displacement.

Furthermore, the pyramid geometry exhibits superior stability compared to traditional cubic or rectangular gabions. This is attributed to a 'nesting' effect, where the tapered sides of the pyramid increase the contact surface area between units, thereby enhancing frictional resistance (F_f). This phenomenon explains why damage remained minimal (below 1%), even when subjected to high wave steepness (H_i/L) under emerged conditions. To validate this structural superiority, the results were compared against established standards; according to the Shore Protection Manual [13], traditional rock armor typically has K_D values ranging from 2.0 to 4.0. In contrast, the pyramid gabions in this study achieved significantly higher K_D values, reaching up to 23.73. This discrepancy stems from the 'flexible-bond' nature of gabions; while individual rocks in rip-rap structures act independently, the stones within a gabion are confined by wire mesh, allowing the entire unit to function as a singular, larger, and more stable mass.

When compared to artificial units such as Tetrapods (K_D = 7.0 – 8.0) or Dolos (K_D = 15.0 – 25.0), the pyramid gabion demonstrates competitive stability, particularly in a two-layer configuration. While studies by Rohani et al. [1] suggested

that the stability of stepped gabions is often compromised at the edges, the pyramid shape tested in this research minimizes edge-stress by providing a smoother transition for wave run-up, justifying the lower damage levels observed. Consistent with the findings of Mahmoudof & Hajivalie [43] on submerged breakwaters, our results confirm that the stability coefficient decreases as the relative water depth (d/h) increases. In this study, K_D dropped to 4.9 under submerged conditions, a trend that aligns with the theory that submerged structures are subject to intensified orbital velocities and lift forces during wave overtopping—a phenomenon visually confirmed in the hydrodynamic documentation (Section 4.3). By integrating these interpretations, it is evident that pyramid-shaped gabions offer an optimal balance between the high stability of complex artificial units and the cost-effectiveness of natural rock structures, making them a viable alternative for sustainable coastal protection.

5. Conclusion

This research investigated the stability of pyramid-shaped gabion armor layers through physical model testing. The results demonstrate that wave steepness (H_i/L) and relative water depth (d/h) are the primary factors influencing the stability coefficient (K_D). It was observed that the pyramid geometry provides superior interlocking, particularly in two-layer configurations. Under emerged conditions ($d/h<1.0$), the structure showed high resilience, whereas under submerged conditions ($d/h>1.0$), the damage slightly increased to 6% due to the combined effects of drag and lift forces.

The calculated K_D values range from 4.9 to 23.73, suggesting that pyramid-shaped gabions are a highly stable and cost-effective alternative for coastal protection. The empirical relationship derived from this study ($K_D = f(H_i/L, d/h)$) provides a practical tool for designing permeable breakwaters. Future studies should consider long-term durability tests of the wire mesh in corrosive marine environments to complement these hydrodynamic findings. Overall, the use of pyramid gabions offers a sustainable solution that balances hydraulic performance with environmental permeability.

5.1. Recommendations

Based on the findings and the limitations identified in this study, several recommendations are proposed for future research. This study shows that under *submerged* conditions ($d/h > 1.0$), damage begins to exceed the 1% tolerance standard. Therefore, simulations need to be carried out on a more extreme wave steepness (H_i/L) range to determine the critical point of total structural failure. Since the stability of the unit is highly dependent on the integrity of the gabion, further research should examine the effect of corrosion or the durability of the wrapping wire on the stability coefficient (K_D) in the long term. With the finding that the K_D value reaches a range of 20.00 to 25.00, it is recommended that a study be conducted to optimize the dimensions of the gabion unit on a prototype scale in the field to verify the relative weight efficiency ($W/\rho_s H_i^3$) that has been found in the laboratory

6. Declarations

6.1. Author Contributions

Conceptualization, M. and A.T.; methodology, M. and A.T.; software, M.; validation, M., S.P., A.T., and H.U.; formal analysis, M.; investigation, M.; resources, M.; data curation, M.; writing—original draft preparation, M.; writing—review and editing, M., S.P., A.T., and H.U.; visualization, M.; supervision, M., S.P., A.T., and H.U.; project administration, M.; funding acquisition, M. All authors have read and agreed to the published version of the manuscript.

6.2. Data Availability Statement

The data presented in this study are available on request from the corresponding author.

6.3. Funding

The authors received no financial support for the research, authorship, and/or publication of this article.

6.4. Acknowledgments

Gratitude is extended to the Faculty of Engineering Laboratory, Hasanuddin University, and the Sulawesi V River Basin Authority (BWS) in Mamuju, as well as to all team members who contributed significantly to the implementation of this research.

6.5. Conflicts of Interest

The authors declare no conflict of interest.

7. References

[1] Rohani, I., Thaha, M. A., & Paotonan, C. (2017). Stability of armor breakwater using rock bags. Journal Techno Entrepreneur Acta, 2(2), 34. (In Indonesian).

[2] Srineash, V. K., & Murali, K. (2015). Pressures on gabion boxes as artificial reef units. Procedia Engineering, 116(1), 552–559. doi:10.1016/j.proeng.2015.08.325.

[3] van der Plas, T., van der Meer, J., Dominguez, E. R., & Bijl, E. (2018). Stability of Very Wide Graded Material, Designed as Breakwater Core, Under Wave Attack. Coasts, Marine Structures and Breakwaters 2017, 1101–1113. doi:10.1680/cmsb.63174.1101.

[4] Fatnanta, F., Pratikto, W. A., Armono, H. D., & Citrosiswoyo, W. (2011). The Stability Characteristics of Sandbag Submerged Breakwater. Makara Journal of Technology, 14(2), 16. doi:10.7454/mst.v14i2.708.

[5] Fatnanta, F., Pratikto, W. A., Armono, H. D., & Citrosiswoyo, W. (2011). Deformation Behavior of Sinking Type Sandbag Breakwater. Jurnal Teknik Sipil, 18(2), 1. doi:10.5614/jts.2011.18.2.3. (In Indonesian).

[6] Grigoris, X. (2019). Stability Optimisation of the top armour row of a breakwater with XblocPlus units. Master Thesis, Delft University of Technology, Delft, Netherlands.

[7] Singh, A. K., Dave, M., Salvi, R., & Juneja, A. (2024). An Experimental Investigation into the Use of Three-Stepped Gabion Walls for Coastal Protection Works Using Acoustic Doppler Velocimeter. International Journal of Geosynthetics and Ground Engineering, 10(1). doi:10.1007/s40891-023-00510-6.

[8] Uray, E. (2022). Gabion structures and retaining walls design criteria. Advanced Engineering Science, 2(2), 127-134.

[9] Hudson, R. Y. (1959). Laboratory Investigation of Rubble-Mound Breakwaters. Journal of the Waterways and Harbors Division, 85(3), 93–121. doi:10.1061/jwheau.0000142.

[10] Van der Meer, J. W. (1988). Rock slopes and gravel beaches under wave attack. Ph.D. Thesis, Delft hydraulics, Delft, Netherlands.

[11] Triatmodjo, B. (2001). Coastal engineering Techniques. Beta Offset, Yogyakarta, Indonesia. (In Indonesian).

[12] Triatmojo, B. (1996) Port, Pelabuhan. Beta Offset, Yogyakarta, Indonesia. (In Indonesian).

[13] CERC. (1984) Shore Protection Manual. CERC, U.S. Army Corps of Engineers, Washington, United States.

[14] Thaha, M. A., Dwipuspita, A. I., & Dharmowijoyo, D. B. E. (2021). S-Curve Rubble Mound Breakwater. ICCOEE2020, ICCOEE 2021, Lecture Notes in Civil Engineering, Volume 132. Springer, Singapore. doi:10.1007/978-981-33-6311-3_105.

[15] Horikawa, K. (1978). Coastal engineering: an introduction to ocean engineering. Pers Universitas, Tokyo, Japan.

[16] Yuwono, N. (201). Planning of Hydraulic Scale Models. Kanisius, Yogyakarta, Indonesia.

[17] Juul Jensen, O., & Klinting, P. (1983). Evaluation of scale effects in hydraulic models by analysis of laminar and turbulent flows. Coastal Engineering, 7(4), 319–329. doi:10.1016/0378-3839(83)90002-9.

[18] Puspita, A. I. D., Thaha, M. A., Pallu, M. S., & Maricar, F. (2020). Effect of wave steepness to relative wave run-up on OWEC breakwater. IOP Conference Series: Earth and Environmental Science, 419(1), 012117. doi:10.1088/1755-1315/419/1/012117.

[19] Sorensen, R. M. (2006). Basic Coastal Engineering. Springer, New York, United States. doi:10.1007/b101261.

[20] Van Der Meer, J. (2021). Rock Armour Slope Stability under Wave Attack; the Van der Meer Formula revisited. Journal of Coastal and Hydraulic Structures, 1, 1–24. doi:10.48438/jchs.2021.0008.

[21] Latham, J. P., Lienhart, D., & Dupray, S. (2006). Rock quality, durability and service life prediction of armour stone. Engineering Geology, 87(1–2), 122–140. doi:10.1016/j.enggeo.2006.06.004.

[22] Baart, S., Ebbens, R., Nammuni-Krohn, J., & Verhagen, H. J. (2011). Toe Rock Stability for Rubble Mound Breakwaters. Coastal Engineering Proceedings, 32, 35. doi:10.9753/icce.v32.structures.35.

[23] Jayewardene, I. F., Golshani, A., & Couriel, E. (2023). Maximum Momentum Flux for Stability Analysis of Model and Prototype Breakwaters. Coastal Engineering Proceedings, 37, 6. doi:10.9753/icce.v37.papers.6.

[24] Burcharth, H. F. (1992). Design of rubble mound breakwaters: Structural Integrity. Proceedings of the International Conference on Coastal Engineering, 4-9 October, 1992, Venice, Italy.

[25] Srineash, V.K., Murali, K. (2021). Hydrodynamic Stability of Gabion Box Reef Breakwaters. Proceedings of the Fifth International Conference in Ocean Engineering (ICOE2019), Lecture Notes in Civil Engineering, Volume 106. Springer, Singapore. doi:10.1007/978-981-15-8506-7_3.

[26] Ferren, V., Magdalena, I., Saengsupavanich, C., Dhiya, M. N. F., Sanitwong-Na-Ayutthaya, S., Chandrasekaran, S., Solekhudin, I., Azis, M. I., & Widowati. (2025). Analytical and Computational Methods for Optimizing Gabion-Pile Coastal Structures. Water, 17(4), 551. doi:10.3390/w17040551.

[27] Triatmodjo, B. (1999). Coastal Engineering. Beta Offset, Yogyakarta, Indonesia. (In Indonesian).

[28] Eldrup, M. R., Lykke Andersen, T., & Burcharth, H. F. (2019). Stability of Rubble Mound Breakwaters—A Study of the Notional Permeability Factor, Based on Physical Model Tests. Water, 11(5), 934. doi:10.3390/w11050934.

[29] Bai, Y., Fang, X., Liu, J., Zhou, Y., Wei, X., & Zhi, H. (2024). Two-parameter wave reflection coefficient for an impermeable breakwater armored with Accropodes. Ocean Engineering, 300, 117476. doi:10.1016/j.oceaneng.2024.117476.

[30] Scheel, H., J. (2013). Sea-Gabion Walls for Tsunami and Flooding Protection, for Fish Farming, and for Protection of Buildings in the Sea. WO2014045132A1, Google Patents, Mountain View, United States.

[31] Vieira, B. F. V., Pinho, J. L. S., & Barros, J. A. O. (2024). Semicircular Coastal Defence Structures: Impact of Gap Spacing on Shoreline Dynamics during Storm Events. Journal of Marine Science and Engineering, 12(6), 850. doi:10.3390/jmse12060850.

[32] Thesnaar, E. (2015). Efficiency of tandem breakwater in reducing wave heights and damage level: a Mossel Bay case study. PhD Thesis, Stellenbosch University, Stellenbosch, South Africa.

[33] Jafari, E., Namin, M. M., & Badiei, P. (2021). Numerical simulation of wave interaction with porous structures. Applied Ocean Research, 108, 1–13. doi:10.1016/j.apor.2020.102522.

[34] Chwang, A. T., & Chan, A. T. (1998). Interaction between porous media and wave motion. Annual Review of Fluid Mechanics, 30, 53–84. doi:10.1146/annurev.fluid.30.1.53.

[35] Sollitt, C. K., & Cross III, R. H. (1972). Wave reflection and transmission at permeable breakwaters. Report No. 147, U.S. Department of the Army Corps of Engineers, Washington, United States.

[36] Rageh, O. S., & Koraim, A. S. (2010). Hydraulic performance of vertical walls with horizontal slots used as breakwater. Coastal Engineering, 57(8), 745–756. doi:10.1016/j.coastaleng.2010.03.005.

[37] Mansard, E. P. D., & Funke, E. R. (1980). The Measurement of Incident and Reflected Spectra Using a Least Squares Method. Coastal Engineering 1980, 154–172. doi:10.1061/9780872622647.008.

[38] Zanuttigh, B., & van der Meer, J. W. (2008). Wave reflection from coastal structures in design conditions. Coastal Engineering, 55(10), 771–779. doi:10.1016/j.coastaleng.2008.02.009.

[39] Goda, Y. (2010). Random Seas and Design of Maritime Structures. Advanced Series on Ocean Engineering (3rd Ed.), World Scientific Publishing, Singapore. doi:10.1142/742.

[40] Sugianto, Tahir Lopa, R., Karamma, R., & Paotonan, C. (2025). Development of Oscillating Water Column Breakwater Model. Civil Engineering Journal (Iran), 11(4), 1268–1292. doi:10.28991/CEJ-2025-011-04-02.

[41] Sugianto, S., Lopa, R. T., Karamma, R., & Paotonan, C. (2023). Wave Reflection in Oscillating Water Column (OWC) Type Breakwater. Zona Laut Jurnal Inovasi Sains Dan Teknologi Kelautan, 4(3), 344–352. doi:10.62012/zl.v4i3.31730.

[42] Koraim, A. S., Heikal, E. M., & Abo Zaid, A. A. (2014). Hydrodynamic characteristics of porous seawall protected by submerged breakwater. Applied Ocean Research, 46, 1–14. doi:10.1016/j.apor.2014.01.003.

[43] Mahmoudof, S. M., & Hajivalie, F. (2021). Experimental study of hydraulic response of smooth submerged breakwaters to irregular waves. Oceanologia, 63(4), 448–462. doi:10.1016/j.oceano.2021.05.002.

[44] Kondo, H., & Toma, S. (1972). Reflection and Transmission for a Porous Structure. Coastal Engineering 1972, 1847–1866. doi:10.9753/icce.v13.100.

[45] Ibrahim, M., Ahmed, H., Alall, M. A., & Koraim, A. S. (2016). Proposing and Investigating the Efficiency of Vertical Perforated Breakwater. International Journal of Scientific & Engineering Research, 7(3), 901–908.

[46] Ko, S. R. (2024). An Experimental Study of Multifunctional Modular Units as Artificial Reefs. Master Thesis, Universitat Politècnica de Catalunya, Barcelona, Spain.